

Article

Enhancing the Fuel Properties of Spent Coffee Grounds through Hydrothermal Carbonization: Output Prediction and Post-Treatment Approaches

Chau Huyen Dang ^{1,2,*} , Gianluigi Farru ^{3,*} , Claudia Glaser ⁴, Marcus G. Fischer ¹ and Judy A. Libra ¹ 

- ¹ Department of System Process Engineering, Leibniz Institute for Agricultural Engineering and Bioeconomy (ATB), Max-Eyth-Allee 100, 14469 Potsdam, Germany; mfischer@atb-potsdam.de (M.G.F.); jlibra@atb-potsdam.de (J.A.L.)
- ² Institute of Waste Management and Circular Economy, Faculty of Environmental Sciences, Technische Universität Dresden, Pratzschwitzer 15, 01796 Pirna, Germany
- ³ Department of Civil and Environmental Engineering and Architecture, University of Cagliari, Via Marengo 2, 09123 Cagliari, Italy
- ⁴ Department of Process and Plant Technology, Brandenburg University of Technology Cottbus-Senftenberg, Burger Chaussee 2, 03046 Cottbus, Germany; claudia.glaser@b-tu.de
- * Correspondence: hdang@atb-potsdam.de (C.H.D.); gianluigi.farru@unica.it (G.F.)

Abstract: The reuse potential for the large annual production of spent coffee grounds (SCGs) is under-exploited in most world regions. Hydrochars from SCGs produced via hydrothermal carbonization (HTC) have been recognized as a promising solid fuel alternative. To increase demand, optimization of the HTC and two post-treatment processes, washing and agglomeration, were studied to improve hydrochar in terms of energetic properties, minimizing unwanted substances, and better handling. HTC experiments at three scales (1–18.75 L) and varying process conditions (temperature T (160–250 °C), reaction time t (1–5 h), and solid content % S_o (6–20%)) showed that the higher heating value (HHV) can be improved by up to 46%, and most potential emissions of trace elements from combustion reduced (up to 90%). The HTC outputs (solid yield—SY, HHV, energy yield—EY) were modeled and compared to published genetic programming (GP) models. Both model types predicted the three outputs with low error (<15%) and can be used for process optimization. The efficiency of water washing depended on the HTC process temperature and type of aromatics produced. The furanic compounds were removed (69–100%; 160 °C), while only 34% of the phenolic compounds (240 °C) were washed out. Agglomeration of both wet SCG and its hydrochar is feasible; however, the finer particles of washed hydrochar (240 °C) resulted in larger-sized spherical pellets (85% > 2000–4000 μm) compared to SCGs (only 4%).

Keywords: spent coffee grounds; hydrothermal carbonization; energy yield; process output prediction; aromatic production; post-treatments; char washing; agglomeration



Citation: Dang, C.H.; Farru, G.; Glaser, C.; Fischer, M.G.; Libra, J.A. Enhancing the Fuel Properties of Spent Coffee Grounds through Hydrothermal Carbonization: Output Prediction and Post-Treatment Approaches. *Sustainability* **2024**, *16*, 338. <https://doi.org/10.3390/su16010338>

Academic Editor: Sandeep Kumar

Received: 17 November 2023

Revised: 11 December 2023

Accepted: 25 December 2023

Published: 29 December 2023



Copyright: © 2023 by the authors. Licensee MDPI, Basel, Switzerland. This article is an open access article distributed under the terms and conditions of the Creative Commons Attribution (CC BY) license (<https://creativecommons.org/licenses/by/4.0/>).

1. Introduction

Coffee production and consumption in the world reached approximately 10 million tons of coffee beans in 2022, and the demand continues to grow each year [1]. Spent coffee grounds (SCGs), one of the major by-products from the production of coffee drinks and other products, are produced in similar quantities, though very decentrally, in locations ranging from home kitchens and coffee shops to instant coffee and drink producers. After brewing or extracting for coffee beverages, SCGs contain a high water content of 50–60 wt%, a relatively high calorific value of 19–22 MJ/kg, and a carbon content of 47.0–60.0 wt% [2–5]. The carbon content includes celluloses, hemicelluloses, lignins, lipids, minerals, and protein, together with phenolic compounds, caffeine, and chlorogenic acids, in addition to nutrients such as calcium, magnesium, potassium, sodium, iron, zinc, manganese, and copper [6–8]. Often, these large amounts of SCGs are disposed of improperly,

which can cause negative effects on the environment, human and animal health, or in landfills, which can cause greenhouse gas (GHG) emissions, besides wasting their potential as a valuable carbon-rich resource. Numerous studies have determined that SCGs can be valorized as a renewable energy source [9,10], as soil amendments [11,12], or in novel materials [13,14]. Nevertheless, the large potential for the reuse of SCGs is underexploited in most regions of the world. This may be due to the difficulties associated with their decentral production and high moisture content, which can lead to molding and biodegradation during the collection and transport stages. In addition, despite their calorific value similar to wood, the use of pure SCGs as fuel, for example for coffee processors, can lead to lower boiler efficiency and increased particle and gas emissions [15].

The thermochemical conversion of these wet SCGs to carbon-rich materials (hydrochars) via hydrothermal carbonization (HTC) has been demonstrated successfully in several studies for fuel utilization [16,17], soil amendment [7,18], and adsorption materials [19,20]. HTC, also referred to as wet hydrolysis or wet torrefaction, is an efficient technology for converting high water content biomass into high-carbon solids with sub-critical water in the temperature range of 180–250 °C under saturated vapor conditions between 10 and 80 bars for a reaction time varying from 1–12 h [21,22]. At these temperatures and times, all pathogens and microbial DNA that developed during collection can be effectively eliminated [23]. The energy content of hydrochar is higher compared to the original biomass [24]. Increases in the higher heating value (HHV) from 19–22 MJ/kg for SCGs and up to 34 MJ/kg for hydrochar have been found [25–27]. These increases depend on the HTC process conditions used and must be considered together with the solid yield (SY) in order to evaluate the energy yield (EY) from the process. The optimal process conditions often must be experimentally determined, but the effort may be reduced through recent advances in modeling [28]. They used genetic programming (GP) to develop models to predict the HTC outputs SY, HHV, and EY as a function of process conditions and feedstock and/or hydrochar composition. Although their data set encompassed an extensive number of feedstock, SCGs were not included.

In addition to hydrochar, a process water and a small amount of gas is produced in HTC. The complex thermochemical degradation and polymerization steps can dissolve inorganics in the feedstock, such as trace elements and nutrients, into the process water, effectively reducing the ash content of the hydrochar and enhancing its energetic properties [29] as well as producing sugars, organic acids, and furanic and phenolic aromatic compounds that transfer to the process water or remain in the hydrochar [30,31]. While many of these compounds in the process water can be transformed into biomethane via anaerobic digestion [32,33], these can be problematic if they remain in the hydrochars when used as solid fuel or soil amendment without post-treatment. Some furanic and phenolic aromatic compounds are considered toxic to humans [34,35] and inhalation or contact should be avoided during hydrochar handling, while some studies have found that these aromatic compounds in the hydrochar can inhibit seed germination when applied to growing media [18,36].

Therefore, in order to increase the efficient use of this resource, post-treatment methods are required to improve the quality and handling of hydrochar as a product. Combinations of processes may be necessary to convert the SCGs into a solid fuel suitable for use in households or industry or into a soil amendment product. One post-treatment method to remove unwanted material from hydrochars is washing. Although a water washing step seems an economical way to wash out unwanted substances if it can be recirculated back to the HTC system, there are very few studies using this method. Most washing tests have been carried out to reduce phytotoxicity from the hydrochar and often do not monitor concentration changes in individual compounds. In their recent review, Karatas et al. (2022) [37] point out that both organics and inorganics could play a role in phytotoxicity, and numerous approaches for its reduction have been tried, ranging from washing and composting to thermal treatment. For example, washing with organic solvents and/or water mixtures was found to reduce organic compounds [38,39], but may require water washing to remove the solvent, depending on the application. The washing of hydrochars

from SCGs has not been deeply investigated. Cervera-Mata et al. (2021) [40] compared the effect of SCG and washed hydrochars on the growth inhibition of lettuce and found little difference, but individual organic compounds were not identified.

Agglomeration is another process that may be useful to improve the physical properties of the hydrochar end product. In addition to the unwanted compounds, hydrochars from SCGs may contain fine particles, which can cause challenges in further handling and transportation. Through agglomeration, the fine particles are bound into larger pellets in order to enhance their flowability and ease of handling and transportation. Extruder pelletizing is one agglomeration type commonly used for producing cylindrical pellets for biomass and its chars [41,42]. For example, dry SCGs and mixtures with other plant-based biomass (e.g., sawdust) were successfully pelletized in an extruder [43,44]. With high water content in both SCGs and their hydrochars, wet agglomeration can be a better process for granulating these materials. However, no studies have tried wet agglomeration for SCGs and their hydrochars. Wet agglomeration is known as a process to enlarge the size of fine particles from wet materials [45,46], which might be possible for producing spherical pellets from the wet hydrochar after HTC.

A review of the literature on HTC shows that most prior research has focused on specific aspects of either the HTC process or post-treatment. However, an investigation of an entire treatment scheme (prediction—optimization—conversion—post-treatment) for HTC using SCGs as feedstock is still underdeveloped. Therefore, this study aimed to fill these important knowledge gaps in the study of SCG valorization from HTC to high-quality end products. Firstly, we explored whether the recently proposed GP models to predict HTC outputs can be used on SCGs, which could help reduce experimental effort for researchers in the future. Secondly, two post-treatments were investigated for their ability to improve product handling characteristics of the hydrochars, washing, and agglomeration. Hydrochar from SCGs was produced in two groups of HTC experiments to identify the significant process parameters on the HTC outputs (SY, HHV, EY): (1) experiments planned with a custom design of experiments (DoE) and (2) random runs at different scales. Three process parameters holding temperature (160 to 250 °C), reaction time (1 to 5 h), and solids content (6 to 20%) were varied. Physical and chemical properties of SCGs, hydrochars, process waters, washed hydrochars, and wash waters were determined. Agglomeration experiments were made using SCGs, three washed hydrochars, and one unwashed hydrochar with plant-based additives and the binder solution of methylcellulose acetate for producing spherical pellets. The size distribution, bulk density, and mechanical stability of spherical pellets were determined and compared to cylindrical pellets of SCGs and their hydrochar.

2. Materials and Methods

2.1. Materials

Spent coffee grounds (SCGs) were collected from canteens and cafeterias at (1) the Dresden University of Technology, Germany and (2) the University of Cagliari, Italy. The initial water content (WC) of collected SCGs was approx. 55 wt%, and then it was dried to a constant water content of 8 wt% at 105 °C for 24 h and stored at 4 °C to avoid biodegradation.

2.2. Overview of HTC Experiments

2.2.1. HTC Reactors

Three different scales of the HTC system were used in this study to convert SCGs into carbon-rich materials. The experiments were performed at ATB using two pressurized stirred reactors of 1 L and 18.75 L (PARR Instrument company, USA (Figure S1a,c in the Supplementary Materials (SM))). These stainless steel reactors were externally heated to various temperatures, including 160 °C, 200 °C, 220 °C, 230 °C, 240 °C, and 250 °C, with reaction times of 1 h, 3 h, and 5 h. The experiments were implemented at the University of Cagliari, Italy using the 1.5 L pressurized unstirred reactor (Berghof GmbH, Eningen, Germany) (Figure S1b in SM) at 220 °C and 240 °C in 1 h.

2.2.2. HTC Experimental Set-Up

Design of the HTC Experimental Set-Ups and Evaluation

Two different sets of experiments were carried out: (1) a random (R) set-up and (2) a Design of Experiments (DoE) set-up. In both set-ups, three input parameters were varied systematically (temperature T , reaction time t , and solid content $\%S_o$). The random set-up was made up of 7 HTC runs (R), whereas the DoE set-up contained 6 HTC runs (D) planned using a custom design of experiments (DoE). The DoE was chosen to design the minimum number of HTC experiments to investigate the main effects of the three variables as well as two-way interactions [47,48]. These experiments were designed and evaluated by using the statistical software JMP (v13.0, SAS) to produce the DoE models, general multiple linear regression equations to describe the main effects of input process parameters, the related two-order interactions, and the quadratic terms. The modeled results were compared with the measured results as well as to literature correlations described in Section 3.1. In addition, the severity factor (SF) was determined based on the HTC operating temperature and reaction time of each run. The severity factor is a useful index that can describe the relationship between the operational conditions of hydrothermal processes [49,50]. The SF is calculated by using following Equation (1):

$$SF = \log (t \cdot e^{[(T - 100)/14.75]}) \quad (1)$$

where:

t = reaction time (min);

T = the operating temperature ($^{\circ}\text{C}$).

Experimental Conditions and Procedure

In total, 13 runs were carried out with SCGs as feedstock using systematic variation of three input parameters at three different reactor scales. Solid content $\%S_o$ ranged from 6 to 20 wt%-db, holding temperatures T were between 160 $^{\circ}\text{C}$ and 250 $^{\circ}\text{C}$, and reaction times t were set from 1 to 5 h. Agitation was held constant for the 6 DoE runs operating in an 18.75 L HTC reactor, while the random set-up included both non-stirred and stirred (90 rpm) runs operating in 1 L, 1.5 L, and 18.75 L reactors. The post-treatment of the hydrochars from the DoE set-up by washing and agglomeration is described below in Section 2.3. Details regarding all experiments within the two HTC set-up groups are presented in Table 1. The code used to designate each experimental run, e.g., D_240_1_13%, contains information on the set-up runs (D-DoE, R-random) and process parameters (T , t , $\%S_o$), while the code for the hydrochar indicates whether it is unwashed (HC) or washed (wHC).

To achieve the desired solid content, deionized water was added to the appropriate amount of dried SCGs in the reactor. After each HTC run, the reactor was cooled down for one hour using cold tap water (1 L reactor) or for 8 h using air (1.5 L and 18.75 L reactors) before gas collection through a valve. The collected gas was then transferred into an aluminum bag, with its volume quantified by using a drum-type gas meter (Ritter GmbH, Bochum, Germany). Subsequently, the percentages of gaseous components (O_2 , CO_2 , CH_4 , H_2S) were determined by using the Biogas 5000 (Geotech company, Coventry, UK). The slurry output was separated through vacuum filtration using flat filter paper (ROTH Type 113A-110, 5–8 μm) into two main products: (1) a solid, known as hydrochar (HC), and (2) a liquid, known as process water (PW). The fresh mass of the filter cake was weighed, and samples were taken from each phase. Each DoE run was conducted once, while the runs of the random set-up were repeated, (1.5 L reactor: 10 times at 220 $^{\circ}\text{C}$; 5 times at 240 $^{\circ}\text{C}$; 18.75 L reactor: 4 times at 220 $^{\circ}\text{C}$, 3 h), aimed at generating a sufficient quantity of hydrochars for subsequent analysis.

Characterization of SCGs and HTC Products

The physical and chemical properties of both the SCGs and HTC products, including hydrochar (HC) and process water (PW), were analyzed. Each sample was measured in

triplicate, from which mean values and standard deviations were derived. For the SCGs, HC and PW, pH, and electrical conductivity (EC) were determined by using the inoLab pH/Cond 720 (WTW, Weilheim, Germany). For solid samples (SCG and HC), the elemental composition (CHNS) was measured using the VARIO EL III (Elementar Analysensysteme GmbH, Germany), with O determined by difference. The assessment of the higher heating value (HHV) was conducted based on the DIN EN 15400:2011 standard using the C200 bomb calorimeter (IKA-Werke GmbH & Co. KG, Staufen, Germany). The ash content was determined at 550 °C, 2 h within a muffle oven CW1113 (Carbolite Gero GmbH & Co. KG, Neuhausen, Germany). Major chemical elements and trace heavy metals were determined through two steps. First, the digestion was made using the ultraClave IV microwave digestion system (MLS Mikrowellen-Labor-Systeme GmbH, Leutkirch, Germany). Then, the analysis was performed by using the iCAP 6000 Series ICP–OES Spectrometer (Thermo Fisher Scientific GmbH, Dreieich, Germany). Aromatic compounds in SCG, HC, and PW were analyzed using the Dionex HPLC UltiMate 3000 (Thermo Fisher Scientific GmbH, Dreieich, Germany). For the extraction of the solid samples, two methods were used: steam distillation (furfural, phenol, cresol, and guaiacol) and water extraction (HMF, catechol). To evaluate the energetic characteristics of the HC with regard to fuel quality assurance, the standard for graded thermally treated and densified biomass fuels meant for commercial and industrial applications (DIN EN ISO 17225-8:2023) served as the framework [51].

Table 1. Summary of HTC runs from two sets, DoE set-up and random set-up. In each set, three process parameters, solid content [wt%-db], temperature [°C], and reaction time [h], were varied.

Set	Runs	Codes		WC _{SCG} [wt%]	Size _{reactor} [L]	%S _o [wt%-db]	HTC Process Parameters			
		Unwashed HCs	Washed HCs				T [°C]	t [h]	a [rpm]	SF [-]
DoE set-up	D_240_1_13%	HC_240_1_13%	wHC_	8	18.75	12.98	240	1	200	5.90
	D_160_5_6%	HC_160_5_6%	wHC_	8	18.75	6.02	160	5	200	4.24
	D_240_5_6%	HC_240_5_6%	wHC_	8	18.75	6.00	240	5	200	6.60
	D_160_1_6%	HC_160_1_6%	wHC_	8	18.75	6.02	160	1	200	3.54
	D_200_3_13%	HC_200_3_13%	wHC_	8	18.75	12.96	200	3	200	5.20
	D_160_5_13%	HC_160_5_13%	wHC_	8	18.75	12.94	160	5	200	4.24
Random set-up	R_230_3_20%	HC_230_3_20%		55	1	20.11	230	3	90	6.08
	R_250_3_20%	HC_250_3_20%		55	1	20.07	250	3	90	6.67
	R_220_1_10%	HC_220_1_10%		55	1.5	10.00	220	1	0	5.31
	R_240_1_10%	HC_240_1_10%		55	1.5	10.00	240	1	0	5.90
	R_200_3_20%	HC_200_3_20%		8	18.75	20.02	200	3	90	5.20
	R_220_3_0%	HC_220_3_20%		8	18.75	20.04	220	3	90	5.79
R_230_3_20%	HC_230_3_20%		8	18.75	20.10	230	3	90	6.08	

WC_{SCG} = water content of SCGs [wt%]; %S_o = solid content in reactor [wt%-db]; T = temperature [°C]; t = reaction time [h]; a = agitation [rpm]; SF = severity factor [-].

2.2.3. Comparative Evaluation of Output Predictions after HTC

Within this study, an assessment was conducted on the predictive capabilities of the DoE model and the graph-based genetic programming (GP) models proposed by Marzban et al. (2022). This evaluation involved a comparison between the predictions generated by these models and the actual measured values for the outcomes, including the solid yield (SY), energy yield (EY), and higher heating value (HHV) of hydrochars. These assessments were performed across varying scales of HTC runs within two experimental set-ups (DoE and random). The aim was to analyze the accuracy and effectiveness of the DoE model and the GP models in predicting the desired outputs derived from different HTC operational conditions and properties of biomass and hydrochar. The correlations for HTC outputs from the DoE model and GP models are listed in Table 2.

2.3. Overview of Washing and Agglomeration Methods

2.3.1. Char Washing

In this experiment, the six wet hydrochars from the DoE runs were washed twice to evaluate their effectiveness in eliminating impurities or soluble substances produced by the carbonization process. Such substances may be detrimental in solid fuel applications within industrial facilities. The two char washings were conducted sequentially for each

char directly after production. The experiment was carried out as follows: (1) Washing step: the filter cake that was separated by vacuum filtration from the HTC slurry (Section 2.2.2) was transferred back to the 14 L filtration unit re-suspended in 8 L of deionized water (33–35 °C) and manually mixed well for 3–5 min. (2) Separation step: the washed hydrochar and wash water were separated by using vacuum filtration and samples of both phases were collected for characterization. (3) Characterization step: the physical and chemical properties (pH, EC, CHNS, HHV, ash content, and aromatic compounds) were measured for both samples to evaluate the effectiveness of the washing process. This procedure was repeated for a second washing round. Details and codes are found in Table 3.

Table 2. Correlations used for predicting HTC outputs: solid yield (SY), higher heating value (HHV), and energy yield (EY) based on the elemental composition of biomass or hydrochar and/or operating conditions. There are equations for (1) calculation of experimental values, (2) DoE model's process-based predictions, (3) GP model's predictions.

Dependent Parameters	Correlations for HTC Outputs (SY, HHV, EY): from DoE Model (This Study) and GP Models (from Marzban et al., 2022) [28]
For calculations from measured values	
SY [wt%-db]	= (mass of HC/mass of FS) * 100% (2)
EY [%]	= SY*(HHV _{HC} /HHV _{FS}) (3)
S _o [wt%-db]	= (mass dry FS/(mass water in FS + mass added water)) * 100% (4)
R [-]	= mass dry FS/mass total water (5)
Developed in this study—DoE models	
SY [wt%-db]	= 103.95 + (−0.24*T) + (0.18*t) + (0.63*%S _o) (6)
HHV [MJ/kg]	= 10.06 + (0.09*T) + (0.37*t) + (−0.02*%S _o) (7)
EY [%]	= 79.57 + (−0.06*T) + (0.99*t) + (0.83*%S _o) (8)
For comparison—GP models	
SY-OP [wt%-db]	based on the operating conditions = 82.96 + 48.95*R − 0.01454*t − 0.0006*T ² (9)
HHV-EA [MJ/kg]	based on elemental composition of the HC (or FS) = 0.3853*C _{char} + 44.98/O _{char} (10)
HHV-OP [MJ/kg]	based on measured HHV ₀ –FS and HTC-operating conditions = HHV ₀ + $\left(\frac{0.51}{R+0.65*HHV_0-10.93}\right) + \left(\frac{T+0.0003*t+T-143.3}{HHV_0}\right)$ (11)
EY-EA [%]	based on the elemental composition of FS and HC (no measured HHV) and SY-OP = (82.96 + 48.95 * R − 0.01454 * t − 0.0006 * T ²) * $\left(\frac{0.3853*C_{char} + 44.98}{0.3853*C_{feed} + O_{feed}}\right)$ (12)
EY-OP [%]	based on measured HHV ₀ –FS value and HTC-operating conditions—using the HHV-OP and SY-OP correlations = (82.96 + 48.95 * R − 0.01454 * t − 0.0006 * T ²) * $\frac{HHV_0 + \frac{0.51}{R+0.65*HHV_0-10.93} + \frac{T+0.0003*t+T-143.3}{HHV_0}}{HHV_0}$ (13)
EY-EA+OP [%]	based on the HHV-EA for FS, HHV-OP for HC and SY-OP correlations = (82.96 + 48.95 * R − 0.01454 * t − 0.0006 * T ²) * $\frac{HHV_0 + \frac{0.51}{R+0.65*HHV_0-10.93} + \frac{T+0.0003*t+T-143.3}{HHV_0}}{0.3853*C_{feed} + O_{feed}}$ (14)

Abbreviations: FS—feedstock, HC—hydrochar, OP—HTC operating conditions, EA—elemental analysis, db-dry basis. T = HTC temperature (°C); t = HTC reaction time (h for DoE model, minute for GP models); %S_o = solid content in the reactor (wt%-db); C_{feed} = carbon content of feedstock (wt%-db); C_{char} = carbon content of hydrochar (wt%-db); O_{feed} = oxygen content of feedstock (wt%-db); O_{char} = oxygen content of HC (wt%-db); HHV₀ = higher heating values of feedstock (MJ/kg); R = mass ratio between dry solid to total water (-).

Table 3. List of selected wet hydrochars and quantity of wash water with the temperature used in the washing experiment.

HCS	m _{HC} [g]	WC _{HC} [wt%]	V _{WW1} = V _{WW2} [L]	T _{WW1} = T _{WW2} [°C]	t _{mix} [mins]	wHCs
HC_240_1_13%	3656.22	74.49	8.00	34.80	3–5	wHC_240_1_13%
HC_160_5_6%	2374.55	76.18	8.00	33.80	3–5	wHC_160_5_6%
HC_240_5_6%	1249.81	70.20	8.00	33.70	3–5	wHC_240_5_6%
HC_160_1_6%	2198.26	77.29	8.00	34.80	3–5	wHC_160_1_6%
HC_200_3_13%	4316.67	76.13	8.00	34.80	3–5	wHC_200_3_13%
HC_160_5_13%	4941.04	78.14	8.00	33.30	3–5	wHC_160_5_13%

m_{HC} = mass of fresh hydrochar (g); WC_{HC} = water content of hydrochar (wt%); V_{WW1} = volume of wash water for first wash (L); V_{WW2} = volume of wash water for second wash (L); T_{WW1} = temperature of wash water for first wash (°C); T_{WW2} = temperature of wash water for second wash (°C); t_{mix} = mixing time for each washing (mins).

2.3.2. Char Agglomeration

Materials and Method

Seven experiments were carried out with SCGs, four wet hydrochars, and various additives to test agglomeration properties. They include three experiments using SCG, two experiments using three washed hydrochars (wHC_160_5_13%, wHC_200_3_13%, and wHC_240_1_13%), and one experiment using a mixture (unwashed hydrochar HC_200_3_20% and washed hydrochar wHC_200_3_13%). Plant-based additives including ground hemp leaves (H, milled to 500 μm), ground corn straw (gS, milled to 500 μm), and corn starch (St) were used in 4 experiments (Exp.2, Exp.3, Exp.5, Exp.6). A solution of 3.8% methylcellulose acetate (M, CAS 9004-67-5) was used as a binder solution (also known as bridging liquid) in 5 of the 7 experiments. Details are listed in Table 4. The water content of the mixture was adjusted to the optimal range of 40–47 wt% in advance. The agglomeration process was conducted using the intensive mixer type EL10 (EIRICH Machines, Inc., Gurnee, IL, USA) shown in Figure S2 in SM. The vessel was operated at a speed of 80 rpm, while the stirring was set at a speed of 1800 rpm. During the agglomeration experiments, the binder solution was sprayed onto the mixture. The length of the mixing time (residence time or dwell time) depended on the time of formation of agglomerated spherical pellets. The experiments were completed once the spherical pellets were formed. Following that, the cumulative distribution Q_3 of particle size was determined, which refers to a statistical representation of pellet size distribution. This parameter was determined by using the AS 200 control siever (Retsch GmbH, Haan, Germany), featuring an amplitude of 1.5 mm, a sieving interval of 10 s, and a duration of 3 min. For measurements of particle size distribution of the initial SCGs, wHC, and HC by using the Mastersizer 3000 (Malvern Panalytical Ltd., Eindhoven, The Netherlands) based on the DIN EN ISO 8130-13 standard, the wHC and HC samples were dried at 105 °C for 24 h and the clumps were broken manually before analysis. The bulk density and mechanical stability of the spherical pellets were also determined. The comparison with cylindrical pellets made from SCG and wHC was also reported in this investigation. The morphology and structure of the spherical pellets were visualized with a VHX 2000 microscope (Keyence GmbH, Neu-Isenburg, Germany). According to Özer et al., 2017 [52], the agglomeration process exhibited two distribution phases as illustrated in Figure 1.

Table 4. Types and masses of materials and additives used in the agglomeration experiments.

Materials, Additives, Binder	TS ₁₀₅	Mass [g-db]						
	[wt%-db]	Exp. 1 (SCG_M)	Exp. 2 (SCG_gSM)	Exp. 3 (SCG_HM)	Exp. 4 (wHC160_M)	Exp. 5 (wHC200_St)	Exp. 6 (Mix_HC 200_St)	Exp. 7 (wHC240_HM)
SCG	96.10	192.20	172.98	172.98				
wHC_160_5_13%	19.70				29.55			
wHC_200_3_13%	95.20					666.40	285.60	
HC_200_3_20%	25.34						51.95	
wHC_240_1_13%	22.80							41.04
Corn starch (St)	96.90					145.35	29.07	
Ground corn straw (gSt)	97.30		19.46					
Ground hemp leaves (H)	95.10			19.02				19.02
Methylcellulose acetate (M)	-	10.26	28.88	28.69	7.60	0.00	0.00	28.12
Total mass of mixture [g-db]	-	202.46	221.32	220.69	37.15	811.75	366.62	88.18
Total mass of water added [g-wb]		267.54	738.68	734.31	312.85	38.25	168.38	851.82
Total mass of mixture [g-wb]		470.00	960.00	955.00	350.00	850.00	535.00	940.00

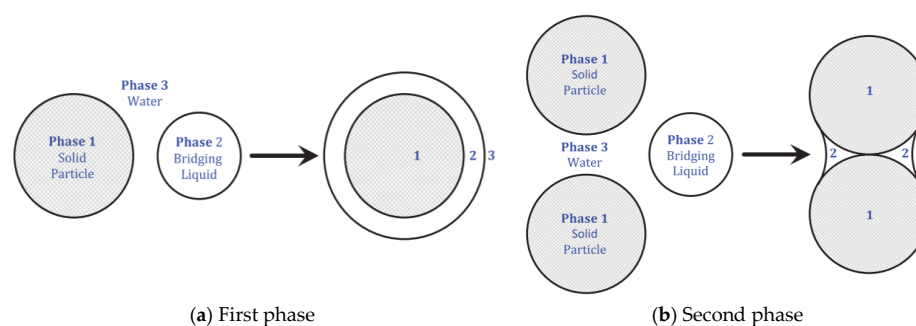


Figure 1. Schematic of wet agglomeration with (a) first distribution phase of wetting and bridging on the surface of material particles and (b) second distribution phase of adhering other particles.

3. Results and Discussion

3.1. Investigating the Impact of Input Variables on HTC Treatment and Predicting Outputs

The impact of three operating parameters, T , t , and S_o , on the HTC treatment of SCGs was determined in an experimental set using a custom design (DoE) with six runs (DoE) and in a second set with seven runs in two different reactor types and sizes with and without stirring (random runs) (Table S1). The contour plots with the experimental results for SY, HHV, and EY and the multiple linear regression equations (DoE models) developed to describe the effect of the T , t , and $\%S_o$ on these HTC outputs are shown in Figure 2a(i–iii). The values for SY and HHV for both the DoE and random runs show the strong dependencies on temperature typically described in the literature, i.e., decreases in SY and increases in HHV with increasing temperature (Figure 2a(i–ii)), which are also found in other studies [18,28,53]. Looking at the DoE models (Figure 2b), it can be seen from the regression coefficients for t that the reaction time has a comparatively small positive effect; variation in t from 1–5 h produced only slight increases in SY and HHV (below 4%). Changes in $\%S_o$ from 6 to 20% affected the values of SY more than the HHV values, causing increases of up to 17% in SY at 250 °C, while HHV remained relatively constant. Previous studies have also reported that HTC temperature is the key parameter influencing the characteristics of the solid fuel [54].

The calculation of the measured EY combines the two outputs SY and HHV; therefore, their inverse relationships with T result in the EY value being more dependent on the $\%S_o$ in the reactor. At low $\%S_o$ (6%), the EY is fairly independent of temperature, remaining mainly below 80% for $T = 160$ – 240 °C; however, as $\%S_o$ is increased to 13%, T plays a larger role and EY decreases with increasing T , having its maximum value 86% at 160 °C (Figure 2a(iii)). At the higher $\%S_o$ (20%), EY is again almost independent of T , with a high of 87.6% at 200 °C. Figure 2c shows that the DoE model predictions of SY, HHV, and EY in both the DoE and random run groups demonstrate a remarkable level of accuracy, closely matching the measured results (AAE = 1.49% (for SY); AAE = 0.89% (for HHV), and AAE = 1.85% (for EY), respectively), even with varying reactor sizes and types. These predictions by the DoE model are valid for HTC runs involving SCGs. They need to be assessed for their ability to predict the HTC outputs for different biomass sources, since the SCGs have already been thermally treated in the roasting (torrefaction) process, in contrast to the other organic feedstocks.

In order to reduce experimental work in the future, the development of predictive correlations to describe the HTC outputs, SY, HHV of the hydrochar, and EY based on operating conditions and the composition of the feedstock, has been the goal of numerous publications [28,49,53,55]. In their recent comparison of a variety of correlations to predict SY, HHV, and EY for 42 mainly lignocellulosic feedstocks based on the HTC operating conditions and/or elemental composition of the feedstock and hydrochar, Marzban et al. (2022) [28] showed that empirical GP-based correlations were able to predict the output values for most feedstock with good agreement. Unlike the DoE models, the GP models for SY and EY predict slightly non-linear dependencies on the reaction temperature. The GP

models for SY and HHV can be combined in a number of ways to predict EY, depending on what information is available, e.g., measured HHV values, the elemental composition of feedstock and hydrochar, and/or operating conditions. The six versions considered here are listed in Table 2. A comparison of the experimental results and predicted values for the three outputs from the GP models, as well as from the DoE model, is shown in Figure 2c (see also Table S1 in SM). It can be seen that the DoE models predict the three output values for both the DoE and random runs with little error (AAE \leq 2%). The GP model SY-OP based on the operating conditions fits the experimental values from both HTC run groups well, though the predicted values are slightly lower (AAE = 4.71%, ABE = -3.90%). This trend of under prediction is continued with the HHV-OP model (AAE = 10.19%, ABE = -10.19%). Thus, when these two parameters are combined in the EY, the EY values are also underestimated to a similar extent (EY-OP, ABE = -13.67% , EY-EA+OP, ABE = -14.58%) In contrast, the GP models that included the elemental analysis of the feedstock and/or hydrochar are closer to the measured results (HHV-EA, AAE = 5.32%, EY-EA, AAE = 6.16%). It is well known that the feedstock properties can have a significant influence on the carbonization products and the energy content of the recovered solids [53,56]. In this case, the underestimation may be due to the size and characteristics of the feedstock; the fine particles of SCGs have already undergone a mild thermal treatment in the roasting process, in contrast to the other feedstocks used to develop the GP models, leading to higher SY and EY than untreated biomass.

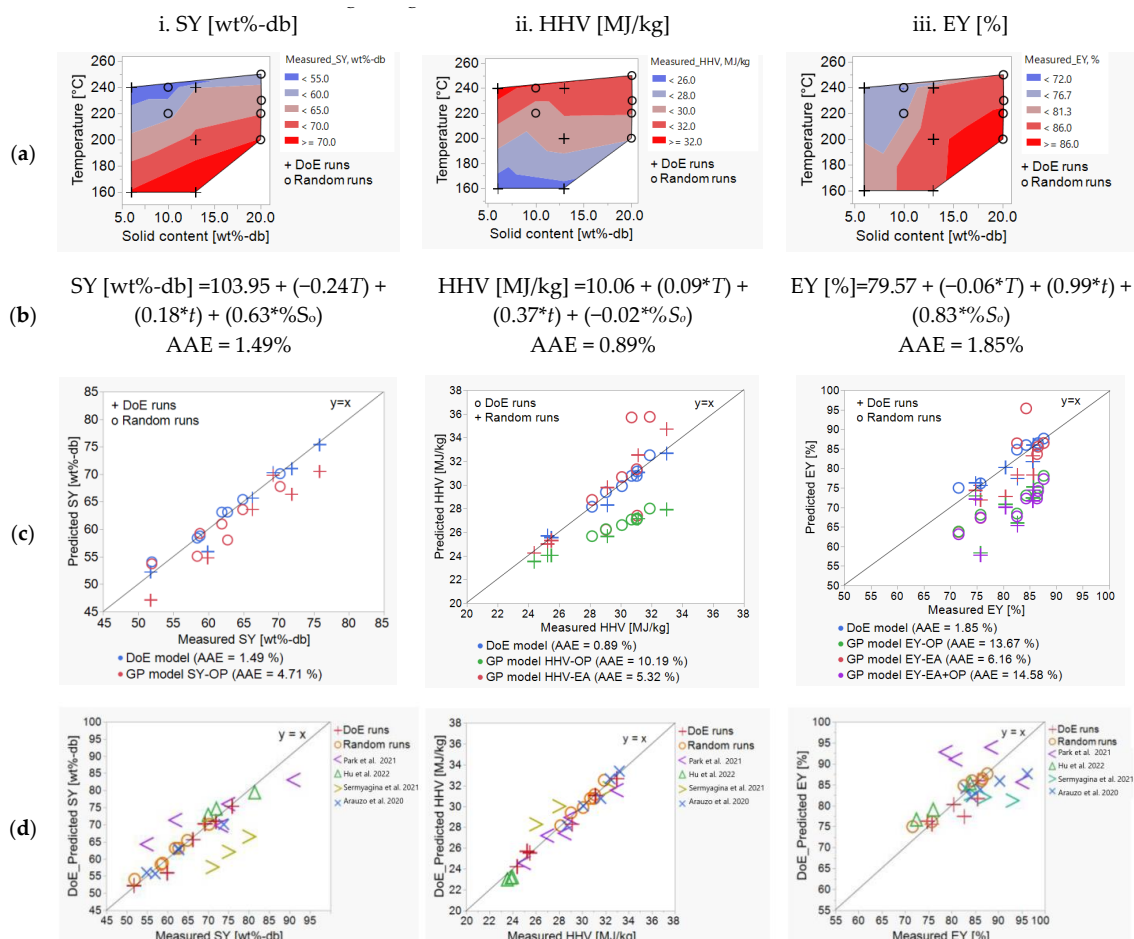


Figure 2. (a) Contour plots showing the dependency of the output parameters on T and S_o for i. SY [wt%-db], ii. HHV [MJ/kg], and iii. EY [%]; (b) equations of the DoE models; (c) comparison of measured and predicted values using the DoE models and the GP models: i. SY-OP; ii. HHV-OP; HHV-EA; iii. EY-OP; EY-EA; EY-EA+OP; (d) comparison of measured and predicted values using the DoE models from this study and the literature (see also Table S2 in SM) [16,17,27,57].

Most modeling efforts based on literature values have limited access to information on feedstock and reactor information. The GP correlations are more generally applicable to a large number of feedstocks due to the inclusion of the properties of biomass and hydrochar in the prediction correlations, but there is room for improvement with more feedstock and reactor parameters. Marzban et al. (2022) [28] note in their study that few results on the effect of % S_o on HTC output are found in the literature; they found only 3 studies out of 35 references in which the solids content was varied over a wide range (1.6–20%), and the trends were highly divergent for SY and EY. The results here contribute to the available data on the influence of % S_o ; however, the thermal pretreatment and small particle size of SCGs will need to be considered when making comparisons. The good agreement between the DoE and random runs shows that the DoE model can be used as an alternative for predicting SCG results. We tested this by predicting values for HTC outputs (SY, HHV, EY) from four literature studies on the HTC of SCGs with 16 different HTC process conditions [16,17,27,57], ranging from T (150–260 °C), t (0.5–3 h), and % S_o (6–30 wt%) with the DoE model (see Table S2 and Figure S3 in SM). Figure 2d illustrates a comparison between the HTC outputs (SY, HHV, and EY) from the literature and those of this study, including both measured and DoE_predicted values. The HHV values from both the literature and this study exhibited a similar trend, with increasing temperatures and reaction times. The values were predicted well with the DoE model (AAE = 3%). In contrast, the SY from two of the four studies were not as well predicted (AAE = 7%), which led to deviations in predicting the EY (AAE = 6%). Further analysis and comparisons are required to better understand the differences.

A practical use for these output correlations is to find the optimal HTC operating conditions to produce hydrochar with the desired fuel characteristics with few or no experiments. To determine the optimal operating conditions for the highest EY, Marzban et al. (2022) [28] suggests solving the correlations for the maximum EY. For the linear DoE model, the maximum EY is found at low T and the highest t and S_o . These trends are visualized in Figure 3a(i–ii). We also explored using the severity factor (SF), which has been developed to combine temperature and time into one factor [49], to describe the effect of processing parameters on the HTC outputs (Figure S4 in SM). However, because the outputs are also highly dependent on the third parameter % S_o , which is not taken into account by the SF, it did not produce an improved correlation. For the non-linear GP models, the high HHV of SCGs represents a special case, so that the calculated EY-OP only decreases with increasing temperature and time (Figure 3b(i)), instead of going through a maximum as T increases, as was seen with feedstocks with lower HHV values [41]. Similar to the DoE, the GP models for EY increase with increased % S_o (Figure 3b(ii)). Therefore, to reach a high EY, the process conditions should be chosen at low T and high % S_o . In a realistic fuel application, the HHV value of the hydrochar may be the primary criterion, with a high EY as a secondary criterion. For example, the values of HHV for the chars produced at 200 °C, 3 h and % S_o from 13–20% are in the range of bituminous coal, with HTC increasing the HHV value of SCGs from 22.5 to 28–29 MJ/kg, while still maintaining a high EY of 85.5–87.6%.

3.2. HTC Treatment: Improving the Energetic Characteristics of Spent Coffee Grounds

HTC treatment has a significant influence on the energetic properties of SCGs, increasing their potential for use as solid fuel. In this study, the HHV was raised from 22.5 up to 32–33 MJ/kg at the highest severity factor (SF = 6.6). These shifts in calorific values are due to changes in the ratios of H/C and O/C, which can give an indication of the composition and structures of organic compounds in hydrochars (see also Table S3 in SM). As the hydrothermal reactions proceed, oxygen-rich functional groups are split off through decarboxylation and dehydration, aromatization, and condensation polymerization, reducing the H/C and O/C ratios [21]. In Figure 4, the left shifting trend of the SCGs to the higher calorific region of more condensed materials such as lignite and anthracite coal is

evident as the severity factor is increased, i.e., the HTC temperatures and residence times are increased.

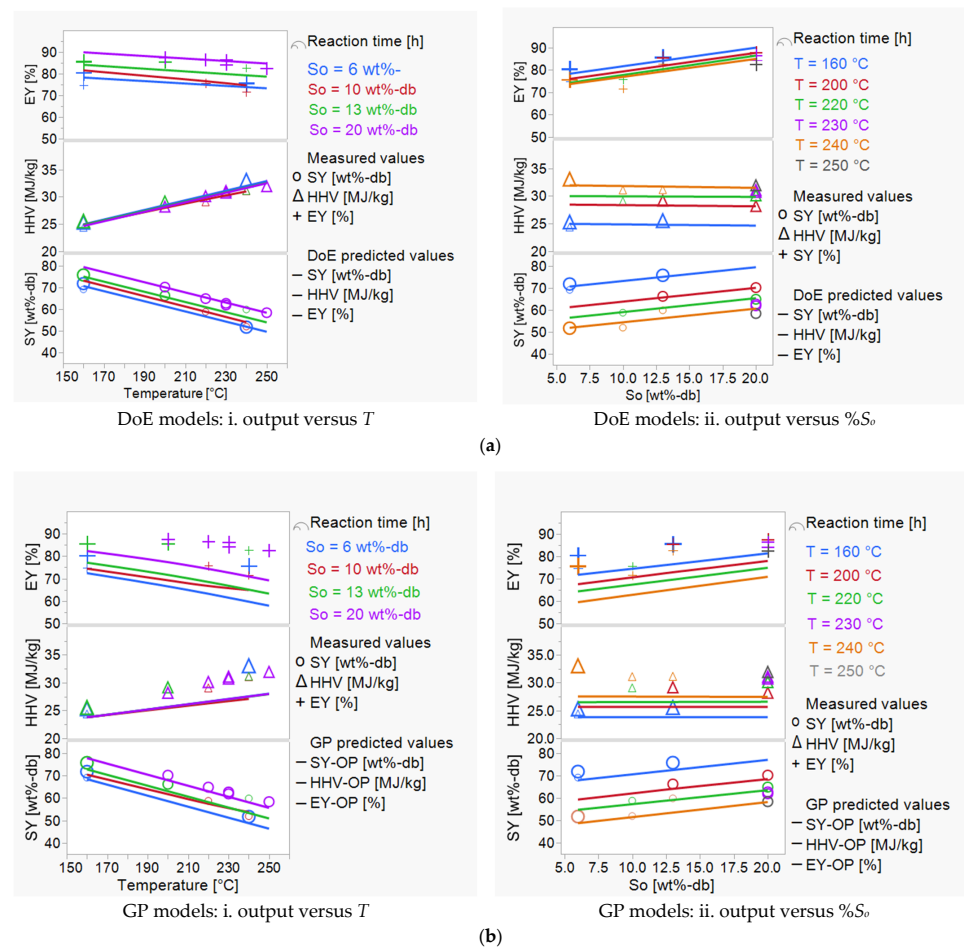


Figure 3. Process optimization with (a) DoE and (b) GP models using the models to predict the HTC outputs, SY, HHV, and EY from T , t , and $\%S_0$ shown as a function of i. temperature T [°C] and ii. solid content in reactor $\%S_0$ [wt%-db].

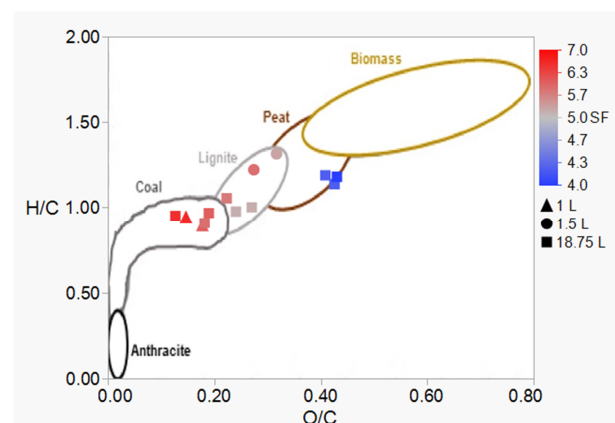


Figure 4. Van-Krevelen diagram with the atomic ratios of H/C and O/C for SCGs and their hydrochars from 13 HTC runs with three reactor sizes at various severity factors (SFs).

Another important parameter for the accurate estimation of air pollutant emissions when burning the fuels is the emission factors defined as the total mass of pollutant emitted per the quantity of energy consumed [58]. According to the standard DIN EN ISO 17225-

8:2023, which applies to thermally treated non-woody biomass fuel, emissions of trace elements such as arsenic (As), cadmium (Cd), chromium (Cr), copper (Cu), lead (Pb), mercury (Hg), nickel (Ni), and zinc (Zn) need to be considered. These are based on the concentration of those elements and the higher heating value of the fuel, and they are reported in mg/MJ. The trace element concentrations in the solids from the DoE runs were measured, except for As and Hg, due to the lack of suitable analytical methods. As can be seen in Figure 5, the elemental emissions caused by all trace elements measured in the SCGs and hydrochars are much lower than the threshold given in the standard. There is a consistent downward trend in the elemental emissions for Cd, Cu, Ni, Pb, and Zn across the majority of hydrochars. Although the SCG values are well below the threshold values, the HTC treatment removed even more of the element, with the exception of Cr. The increase in Cr is probably due to leaching from the stainless steel reactor, and to a lesser extent Ni. This could be avoided through the use of a liner in the HTC reactor.

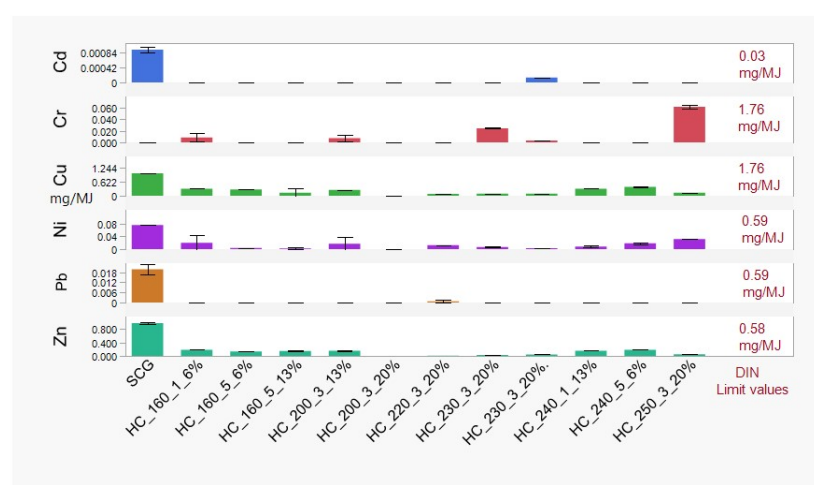


Figure 5. Estimation of emission factors for trace elements such as Cd, Cr, Cu, Ni, Pb, Zn during combustion of SCGs and their hydrochars.

3.3. HTC Post-Treatment: Washing to Remove Simple Aromatics

After the HTC process, the solids are usually suspended as a slurry in the process water and are separated by filtration. The filter cake still retains a large amount of process water (e.g., 70–78% of WC) that may contain inorganic and organic compounds that are unwanted or harmful in the final product. Often, furanic and phenolic compounds are produced in the HTC process, which may be a benefit if the goal is to recover these compounds from the process water as part of a biorefinery strategy [59]; however, if the goal is to produce safe-to-handle hydrochars, these compounds should be avoided or removed. The results of the DoE runs are evaluated in this section first for the potential to choose process conditions to avoid or minimize aromatic production and second for the feasibility of adding a simple washing step to remove the aromatics from the chars.

3.3.1. The Production of Simple Aromatic Compounds in the HTC Process

During hydrothermal carbonization, furanic and phenolic compounds were produced that remained in the process water and/or hydrochar at the end of the carbonization reactions. Furanic compounds, e.g., HMF and furfural, are produced through the dehydration of sugars, while phenolic compounds, e.g., phenol, cresol, catechol, and guaiacol, generally result from lignin degradation [60]. Figure 6 shows the concentrations of the individual aromatic compounds measured in the hydrochar and process water for the DoE runs (see also Table S5 in SM). The HMF concentration in both the hydrochar and process water was generally higher than those of furfural, except at 240 °C. Park et al. (2022) [61] also found similar behavior from the hydrothermal treatment of SCGs at 120–210 °C; more HMF was produced than furfural, reaching the maximum concentrations at 210 °C. The

process temperature has a larger effect on the concentrations than the reaction time or solids content. At 160 °C, the furanic compounds dominate in both the hydrochar and process water (e.g., HC_160_5_6%, in HC: 2474.5 mg/kg-db (HMF) and 2193.2 mg/kg-db (fufural); in PW: 489.5 mg/L (HMF) and 253.6 mg/L (fufural), respectively), while at 240 °C the phenolic compounds are present at high concentrations in both phases (e.g., for HC_240_1_13%, catechol in HC: 1730.2 mg/kg-db, and in PW: 213.8 mg/L). The trends with temperature for the two groups of compounds show an inverse relationship.

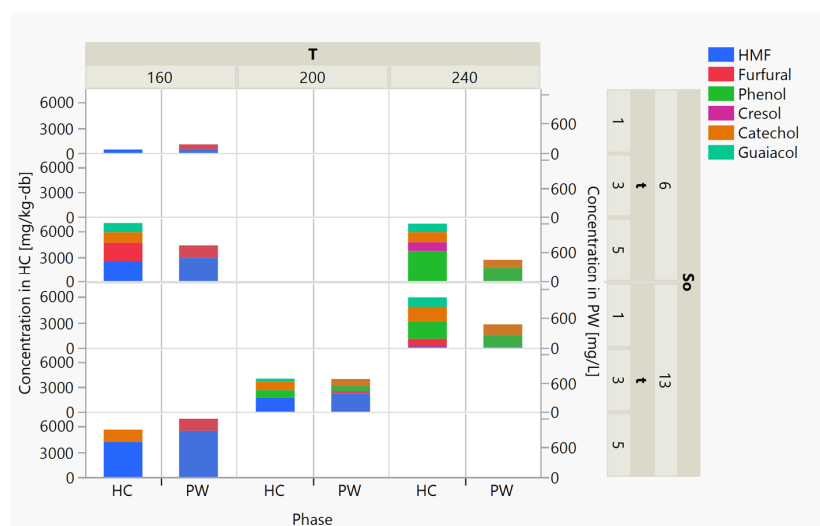


Figure 6. Comparison of the individual aromatic compounds measured in the hydrochar (HC) and process water (PW) under the different process conditions: T , t , S_o .

It is interesting to note that furfural was present in the SCG feedstock at a low concentration, 245 mg/kg-db. Indeed, it is classified as a food flavoring agent when used at low concentrations (below 0–0.5 mg/kg body weight) (WHO/JECFA). The aromatic compounds that develop during the coffee roasting process contribute to the flavor and aroma of the final coffee beverage [62]. Many simple phenols, including phenol, guaiacol, and catechol, and their derivatives are formed in the roasting process primarily from the pyrolysis of chlorogenic acids rather than lignins at low concentrations between 200–300 µg/kg [63]. This is usually an order of magnitude lower than the concentrations found in hydrochar, which range from non-detected to 3690.8 mg/kg-db (phenol). In contrast, higher concentrations of HMF were found in coffee samples (51–1143 mg/L [61]) and in roasted coffee beans (0–600 mg/kg [64]; 7.3–897.0 mg/kg [65]), in addition to furfural (3.0–219.0 mg/kg [65]). The HMF concentrations in the process water remained below the maximum value found in the cup of coffee, staying between non-detected and 938.7 mg/L. In the hydrochar, the HMF and furfural concentrations were often higher than in the coffee beans by an order of magnitude, ranging from non-detected to 4181.4 mg/kg-db (HMF) and 2193.2 mg/kg-db (furfural). Since high amounts of these aromatic compounds are undesired during the handling of the hydrochars due to potential environmental emissions or effects on human health [66], avoiding their production in the HTC process or their removal through the process of washing the char are discussed further.

As already noted, the results from this small DoE study show that the process temperature has a larger effect on the aromatic concentrations than the reaction time or solids content. However, to gain more insight and expand these conclusions, the results are compared to those made in a much larger kinetic study on the effect of the individual process parameters on aromatic production [30]. In their study on two lignocellulosic feedstocks (poplar, wheat straw) and cellulose, sampling over reaction time (0–8 h) for three holding temperatures (200, 230, 260 °C) and constant % S_o (11.1%), Reza et al. (2014) [30] found non-linear trends in the production of aromatic concentrations in process water

for the two lignocellulosic feedstocks, which are significantly influenced by both T and t . The comparison of the results show that more phenolic compounds were produced at the higher temperatures and initially increased with reaction times (Figure 7a,b), similar to SCGs for $t \geq 1$ h. The opposite trend was found for the furanic compounds in the process water for $t \geq 1$ h, except for the samples taken below 1 h. This may be due to the production of furanic compounds during the heating phase, which reacted further at high temperatures and as reaction times increased, leading to little to no furanic compounds being detected at 230–260 °C for $t > 1$ h. At the lower temperature (200 °C), Figure 7b shows that the production of furanic compounds requires a longer reaction time, in line with the results at 160 °C of this study. These non-linear trends are corroborated by Borrero-López et al. (2018) [67] in their extensive HTC kinetic study on the effect of reaction severity on the degradation of hemicellulose, cellulose, and lignin and the production of aromatic compounds. They found similar increases in HMF in process water from cellulose at 160 °C with reaction time, while at 240 °C with hemicellulose the high HMF concentration at $t = 0$ h decreased rapidly with reaction time. In contrast, phenolic concentrations from lignin increased almost exponentially with reaction severity. They proposed two groups of models from their results: kinetic models for the production HMF and furfural for each of the three biomass components and models as a function of the severity factor SF for nine individual phenolic compounds in process water from lignin (Table S6 in SM). The biomass composition was not measured in our study, so their models of two compounds, phenol and guaiacol, are compared to experimental concentrations from our study and from Reza et al. (2014) [30] in Figure 8. The experimental values are lower for guaiacol than the model values and much higher for phenol, although Borrero-López et al. (2020) [31] found good agreement for these compounds between their model and experimental values from the HTC of lignocellulosic biomass, olive stones, and beech wood over a similar range of SF. Unfortunately, it seems that additional factors other than SF must be considered to be able to predict the phenolic concentrations. Nevertheless, knowledge of these inverse trends can help in choosing process conditions depending on the goal. For example, to choose the best conditions for a high EY from SCGs, these aromatic trends can be considered along with the DoE model for EY (Figure 9). Both the EY as well as the sum of aromatic compounds was the lowest at low temperatures and reaction times. More studies are required to develop a practical reliable model for a wide range of feedstock.

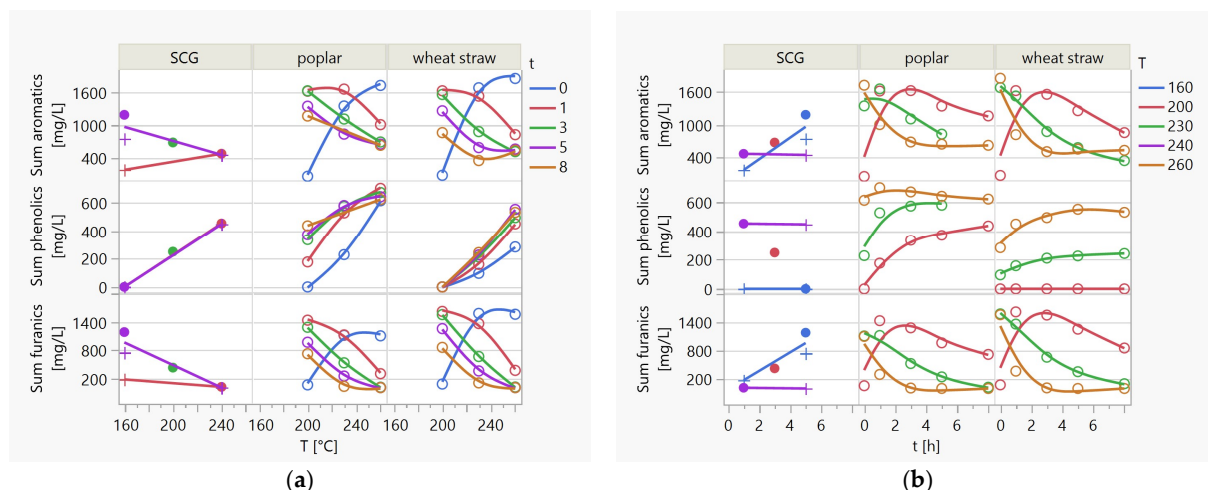


Figure 7. Comparison of the two groups of aromatic compounds, furanic and phenolic, measured in the process water from the HTC of SCGs (DoE runs, this study; $\%S_0 = 6\% +, 13\% \lambda$) with literature values from Reza et al. (2014) [30] for poplar and wheat straw ($\%S_0 = 11\%$, \circ) as a function of (a) holding temperatures T and (b) reaction times t .

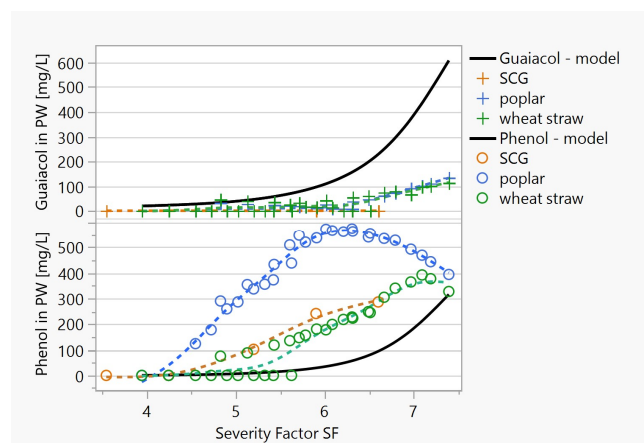


Figure 8. Comparison of the experimental values for guaiacol and phenol in process water from the HTC of SCGs (DoE runs, this study), poplar, and wheat straw (Reza et al., 2014) [30] to values calculated from the model developed by Borrero-Lopez et al. (2018) [67] from the HTC of lignin.

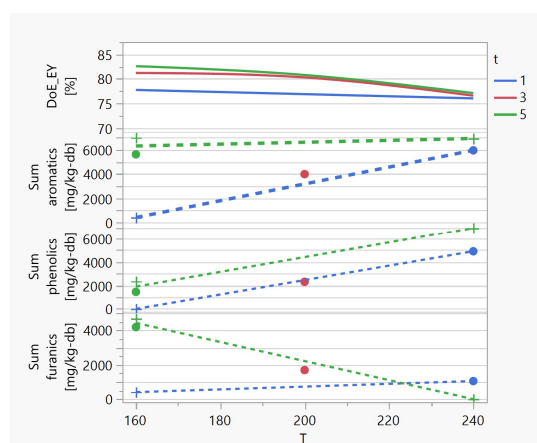


Figure 9. Parameters for the optimization of HTC process conditions for SCGs as a function of temperature, considering EY (predicted with the DoE model) and the experimental values for the sum of the six aromatics in hydrochar from the HTC of SCGs (DoE runs, this study; $\%S_0 = 6\% +, 13\% \lambda$).

3.3.2. Char Washing

The amount of aromatics removed in the two washing steps with hydrochar and water at 30 °C varied depending on the HTC process temperature and type of compounds (Figure 10). The significance of the aromatic concentration changes due to char washing was confirmed using a one-way ANOVA analysis (p -value ≤ 0.05), except for catechol. For the hydrochar produced at 160 °C, 74–100% of the total aromatics were washed out, whereas at 240 °C only 12–34% were removed. The difference is due to the type and amount of compounds produced at the different HTC temperatures, as discussed in the previous section. For instance, furanic compounds, which were present in larger amounts at 160 °C, were washed out successfully (69–100%), while in hydrochar with high concentrations of phenolics (240 °C—5 h), a removal of only 34% was achieved, or the concentration even increased (240 °C—1 h, cresol). It is interesting to note that HHV was not affected by washing. HHV remained the same for all washed hydrochars (see Table S8 in SM). Looking at the changes in the concentrations in the wash water (Figure 10), it can be seen that the concentrations in the two consecutive wash waters decreased drastically, approaching zero in the last wash water (see also in Table S7 in SM). This indicates that further washing under these conditions has little prospect of success.

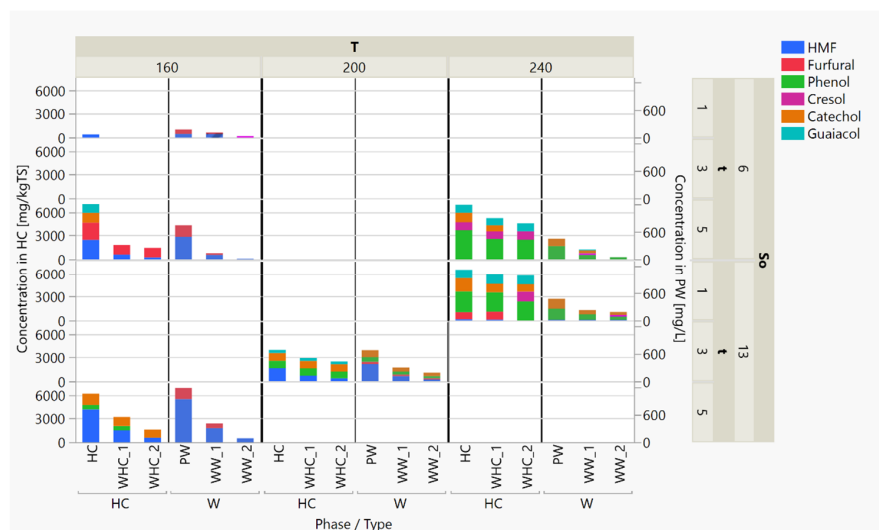


Figure 10. Reduction in the amount of aromatics in hydrochars from two washings with water: comparing the original hydrochar (HC) to the two washed hydrochars (wHC_1, wHC_2) and original process water (PW) to the two wash waters (WW_1, WW_2).

The comparison of the % mass of HMF and phenol in hydrochar after production to that recovered after two washings in the wash waters and in the hydrochar can be seen in Figure 11 for the runs D_160_5_13% (Figure 11a) and D_240_1_13% (Figure 11b). The calculations are based on the mass balance considering the hydrochars and wash waters, and the difference between the input and output is shown as loss. There is a dramatically decreasing trend in HMF mass in hydrochars after each washing, with approximately 88% of HMF mass washed out from the original hydrochar. In contrast, the % mass of phenol in hydrochar decreased only slightly after each washing, with the result that only 15% of the phenol mass was removed from the original hydrochar. These differences between the % mass of HMF/phenol in HC and wHC are significant based on the Tukey–Kramer test (different uppercase letters (A, B, C) indicate significance at $p < 0.001$ levels).

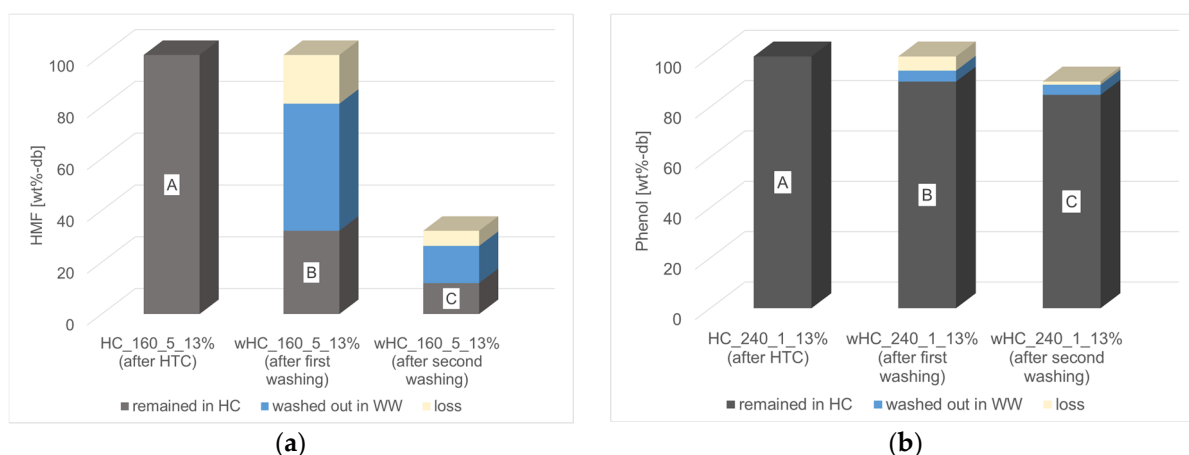


Figure 11. Comparison of the % mass of HMF and phenol in hydrochar after production and recovered after two washings in the wash waters and in the hydrochar; (a) % mass of HMF in HC and wHC from run D_160_5_13%; (b) % mass of phenol in HC and wHC from run D_240_1_13%. (The different uppercase letters indicate significant differences between the HMF/phenol % mass in HC and wHC at $p = 0.0003$ for phenol and $p < 0.001$ for HMF, based on the Tukey–Kramer test.)

In comparison, Chakrabarti et al. (2015) [38] found a high degree of reduction for phenol (96%) when the hydrochar from rice husks was washed with acetone followed by

two water washes, as well as high degrees for furfural (79%) and HMF (96%). This reduction in phenol is much higher than that found in this study (34%); however, a large portion of the rice husk hydrochar was also lost by the three-step washing (35–57%). Washing hydrochar from date palms with water caused a 19% loss in mass, but made almost no change in the mostly water-insoluble polyaromatic hydrocarbon concentrations in the hydrochar [68]. Unfortunately, mass loss from washing was not measured in our study and should be further investigated. For fuel applications, these large losses of mass accompanied by the production of a large volume of wash water to be treated is hardly sustainable, both economically and environmentally. Only one washing study with water and hydrochars from SCGs could be found in the literature; however, the focus was on comparing the effect of the washed hydrochar versus SCGs on plant growth [40]. They found little difference between SCGs and washed hydrochar; both had an inhibitory effect on lettuce growth. No comparison between unwashed and washed hydrochar was made, nor were individual organic compounds identified. These results highlight that more systematic studies on washing should be carried out, coupled with optimizing the process conditions to avoid the production of the aromatics, if possible.

3.4. HTC Post-Treatment: Agglomeration

The agglomeration of the fine hydrochar particles into larger-size pellets is an important step in order to improve the handling and transportation of the hydrochars as fuel or as soil amendments. Since the particle size of the starting materials is a critical factor in an effective agglomeration process [69], the particle size distributions of the feed-stock SCGs and washed and unwashed hydrochars were analyzed (Table 5). Although SCGs are finely ground, only 10% of the particles in this study have diameters less than 150 μm (d_{10}), with 80% falling within the range 150–800 μm (d_{10} – d_{90}). After HTC conversion and filtration from the HTC slurry, the particles became even smaller, with d_{10} decreasing to <50 μm . Similar results for hydrochar from SCGs were found by [16,40]. As HTC temperatures increased, there was a significant reduction in hydrochar particle sizes, most likely due to devolatilization and depolymerization reactions [27]. The size for 90% of the particles of hydrochar particles (d_{90}) was reduced by approximately 84%, from 885 μm (at 160 $^{\circ}\text{C}$) to 141 μm (at 240 $^{\circ}\text{C}$) (Figure 12a,b). Although Park et al. (2021) [16] also found that the larger particles (>500 μm) disappeared as the HTC temperature was raised from 170–250 $^{\circ}\text{C}$, the major gain was in particle sizes between 100–500 μm , with only small increases seen below 100 μm . The subsequent washing step reduced the particle size even more, as can be seen for washed hydrochar (wHC_200_3_13%) compared to unwashed hydrochar (HC_200_3_20%) at similar process conditions (Figure 12a).

Table 5. The results of particle size distribution within materials and additives used in agglomeration experiments. This analysis uses percentiles such as d_{10} , d_{50} , and d_{90} , which represent the particle size below which a certain percentage of the particles fall.

Materials	Particle Size Distribution		
	d_{10} [μm]	d_{50} [μm]	d_{90} [μm]
SCG	150.00	335.00	800.00
wHC_160_5_13%	31.00	406.00	885.00
wHC_200_3_13%	14.30	111.00	437.00
HC_200_3_20%	50.00	290.00	525.00
wHC_240_1_13%	13.70	36.10	141.00
Corn starch	7.20	14.40	22.70
Ground corn straw	29.60	166.00	501.00
Ground hemp leaves	4.80	20.90	75.50

d_{10} (10th percentile) means the size below which 10% of the particles fall; d_{50} (50th percentile) means the size below which 50% of the particles fall; d_{90} (90th percentile) means the particle size below which 90% of the particles fall.

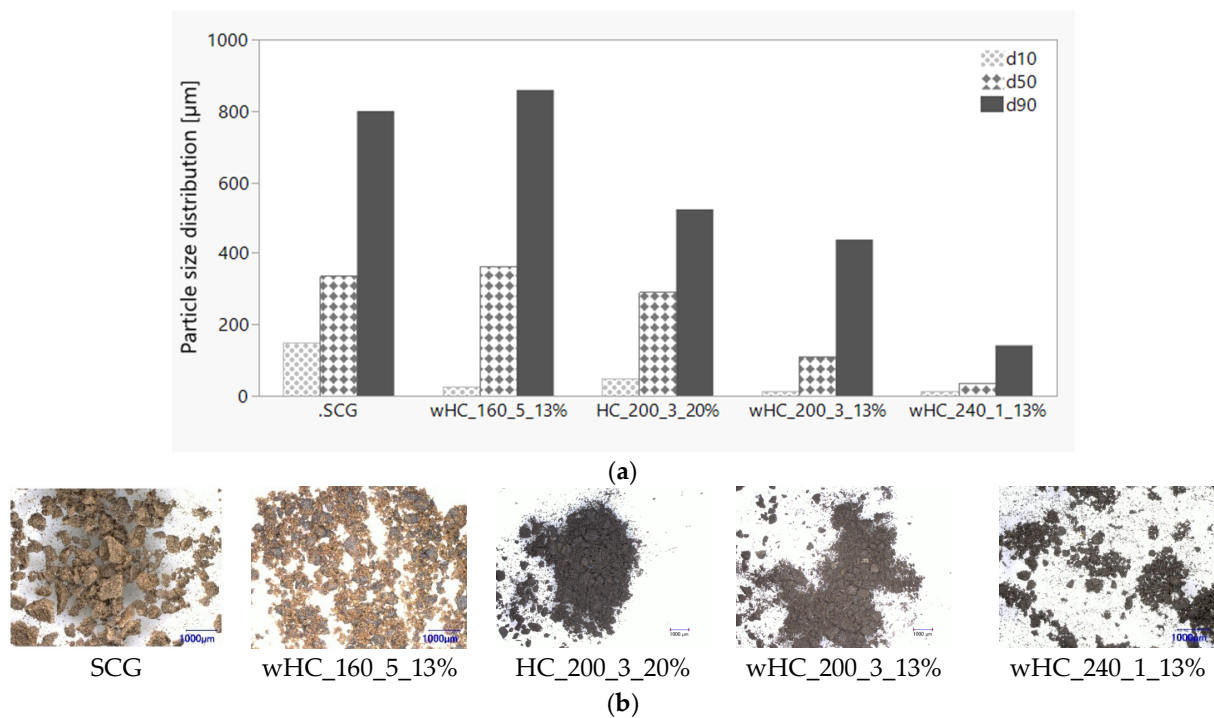


Figure 12. Initial materials including SCG, wHC, and HC used in agglomeration experiments; (a) particle size distribution; (b) images of particles in materials.

After determining the particle size of the starting materials, seven agglomeration experiments to produce spherical pellets were carried out using SCGs, three washed (wHC) and one unwashed hydrochar (HC) with three plant-based additives, and a binder solution of methylcellulose acetate (see Table 4 for compositions). The differences in the sizes of the spherical pellets obtained for each of the starting materials are visualized in Figure 13, which illustrates the cumulative distribution Q_3 of successfully formed spherical pellets from both SCGs and their hydrochars (measured values are provided in Table S9 in SM). In general, the particle size distribution of the starting products has a decisive influence on the pelleting behavior. It is also important that there is a particle size distribution (no monoparticles). The results here show that the coarser the starting material, the smaller the size of the pellets produced, irrespective of the additive used. Over 70% of the spherical pellets produced from SCG are 1000 µm or smaller in size (Exp. 1–3) (Figure 13, dashed lines). A similar pattern was observed with hydrochar in Exp. 4 (wHC160_M) and Exp. 6 (Mix_HC 200_St) (Figure 13, solid lines). In both of these experiments, a significant number of spherical pellets measuring 1000 µm or less in size were obtained, comparable to what was observed using SCGs. This behavior can be attributed to the coarser particles present in the starting materials. In contrast, the agglomeration tests with the starting materials with finer particles (washed hydrochar made at the higher temperatures 200 °C and 240 °C with $d_{10} < 15$ µm) resulted in the production of larger pellets, e.g., in Exp. 7, wHC240_HM, 85% of the pellets fell between 2000–4000 µm (Figure 13, black solid line). The washing of the hydrochar may also play a role here, increasing the wettability of the particle surface with the binding agent (M). Only when a degree of saturation of approx. 80% is reached do the binding adhesion forces/capillary forces act against the separating shear forces in the mixer. The high speeds of the agitator (1800 rpm) promote the particle–particle collision and thus the effectiveness of the binding forces. The duration of the pelletizing process is also decisive for the agglomerate size. Here, a longer dwell time is positive for the formation of larger pellets. However, the following effect also occurs: the simultaneous compaction of the pellet structures can cause pelletizing liquid to escape onto the particle surface, which then leads to the optimum degree of saturation being exceeded

(“wet” surface) and promotes the formation of secondary pellets (i.e., pellets from pellets). Therefore, a material-specific optimum is necessary. Figure 14 shows microscopic images of agglomerated spherical pellets, highlighting variations in size and shape among spherical pellets from SCG, wHC, and a wHC and HC mixture.

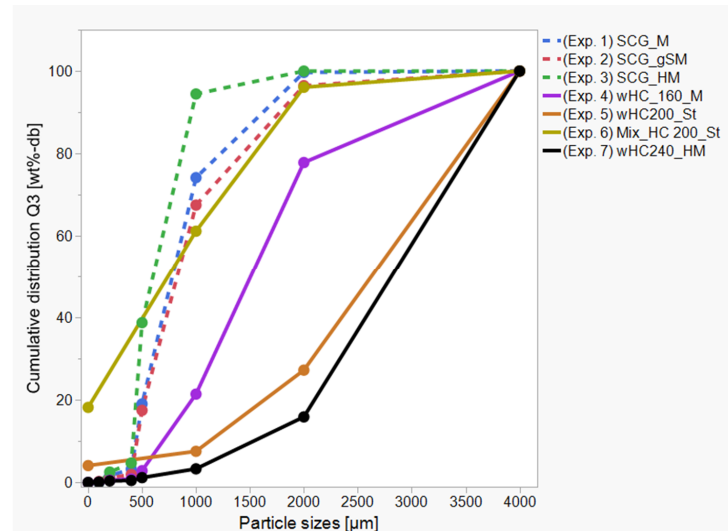


Figure 13. Cumulative distribution (Q3) of the particle sizes of agglomerated spherical pellets produced from SCGs (Exp. 1, 2, 3; visualized by dashed lines), from wHC (Exp. 4, 5, 7), and from a mixture of wHC and HC (Exp. 6) (visualized by solid lines) with plant-based additives (hemp leaves (H), ground corn straw (gS), corn starch (S), and a binder solution of methylcellulose acetate (M)).

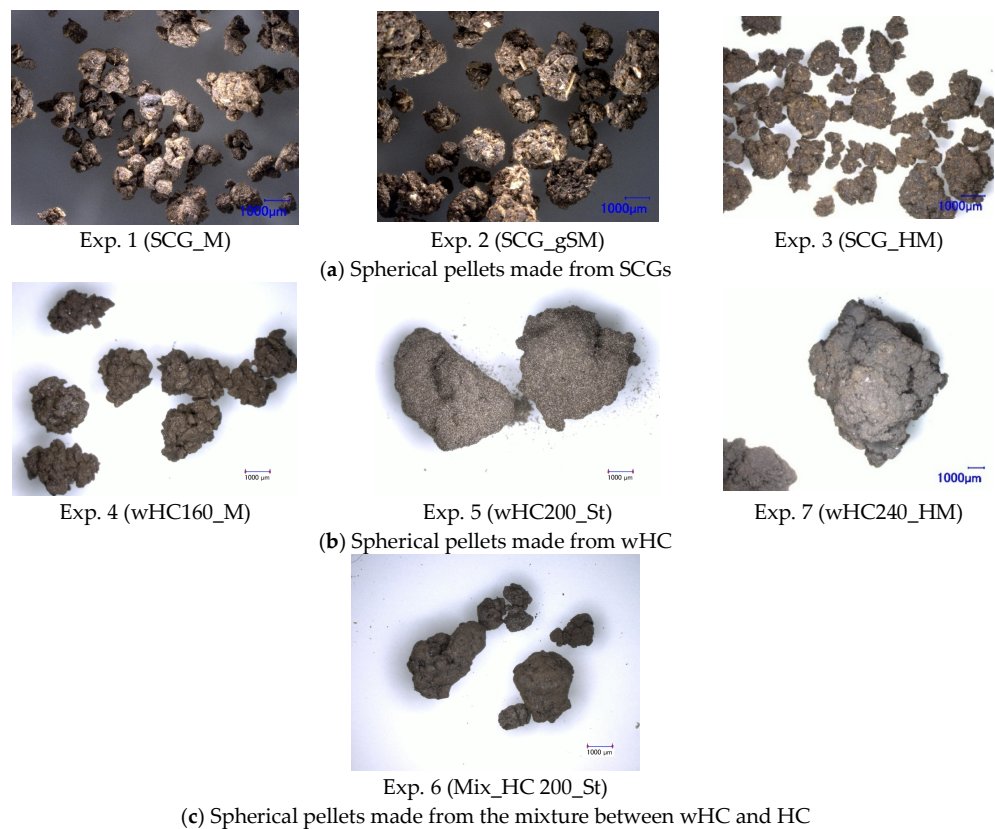


Figure 14. Microscopic images of agglomerated spherical pellets from (a) SCGs, (b) wHC, (c) the mixture between wHC and HC with plant-based additives (hemp leaves (H), ground corn straw (gS), corn starch (S), and a binder solution of methylcellulose acetate (M)).

Following the agglomeration experiments, both bulk density and mechanical stability were determined for the spherical pellets (sp) from four experiments with adequate quantities of pellets: Exp. 2 (SCG_gSM), Exp. 4 (wHC160_M), Exp. 6 (Mix_HC 200_St), and Exp. 7 (wHC240_HM). These two parameters are important to evaluate the performance of pellets during handling, transportation, and storage and are regulated for cylindrical pellets, e.g., in the international standard (DIN EN ISO 17225-8:2023) for pellets derived from thermally treated non-woody biomass. It is worth nothing that there is currently no regulation specifically for spherical pellets. For comparison, cylindrical pellets (cp) produced using an extruder from wood, SCGs, and their HC_220 and wHC_220 were also produced and compared to the standard values. The bulk density values for the four tested spherical pellets were approximately half those of the cylindrical pellets (Table S10 in SM), ranging between 262.50–335.81 kg/m³, which is well below the threshold set by the standard for cylindrical pellets (Figure 15a). Overall, the mechanical stability of all spherical pellets was enhanced, exceeding that of all cylindrical pellets by 10%. However, only spherical pellets from three experiments, Exp. 2 (SCG_gSM), Exp. 4 (wHC160_M), and Exp. 7 (wHC240_HM) using the binder solution, meet the threshold of the standard of 96 wt%-db (Figure 15b). In contrast, the mechanical stability of spherical pellets from Exp. 6 (Mix_HC 200_St) remains below the threshold (Figure 15b), likely due to the addition of corn starch during agglomeration, which can lead to fragility in spherical pellets.

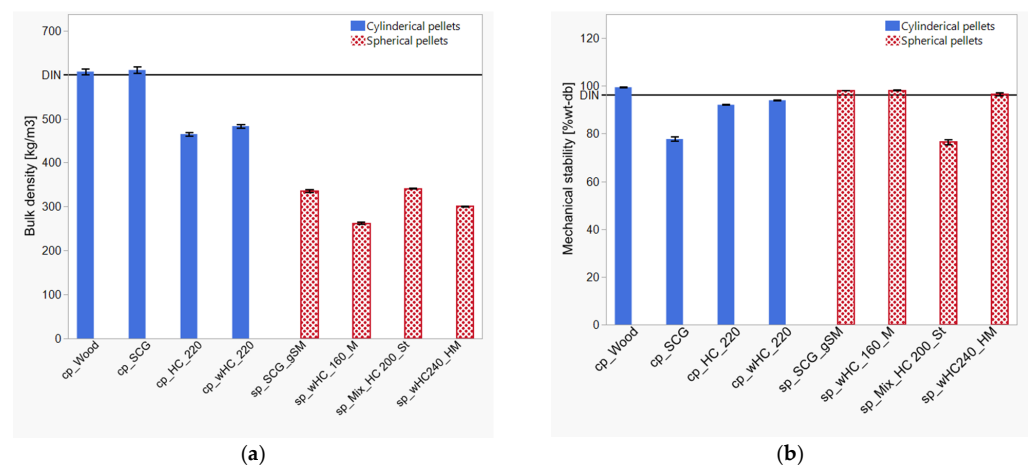


Figure 15. Physical tests for spherical pellets (sp) and cylindrical pellets (cp) and a comparison with the standard (DIN EN ISO 17225-8:2023): (a) bulk density and (b) mechanical stability (standard deviation from $n = 4$).

The initial results from these trials indicate the feasibility of using wet agglomeration to produce spherical pellets from hydrochars from SCGs that are resistant to physical stress, deformation, or breakage. The improved mechanical stability was achieved with a binder solution of methylcellulose acetate. The target size of the pellets as fuel will depend on the requirements of the combustion and handling system. The production of spherical pellets may be very interesting for use in soil amendments, since the size of the hydrochar spherical pellets falls within the target range that most manufacturers aim for in fertilizer granules (2000–4000 μm) to have consistent flow rates [70]. However, for a comprehensive assessment of pellet quality, further investigations are needed to better understand the relationship between the properties of starting materials and the processing parameters of agglomeration.

4. Conclusions

Hydrochar production and properties, output predictions, and process optimization: HTC proved effective in enhancing the energetic properties of SCGs, converting them to hydrochar with a higher HHV and making them suitable for use as solid fuel. In addition,

HTC reduced the concentration of trace elements, which can lead to a reduction in their emissions during combustion of these hydrochars. The predictive models to describe the HTC outputs, SY, HHV of the hydrochar, and EY based on operating conditions (T , t , % S_o) and/or the composition of the feedstock and hydrochar, performed well for all reactor scales tested (1, 1.5, and 18.75 L). Both the DoE model developed here from the experimental results and the published GP models [28] can be used in order to reduce experimental work in the future. For example, the models can be used to optimize the operating conditions to achieve the highest EY from SCGs.

Aromatic production and removal by washing with water: The production of six aromatic compounds, two furanic and four phenolic compounds, during HTC showed inverse trends for the two groups with temperature. The use of char washing as a post-treatment to reduce the aromatic content of the hydrochar was only successful for the furanic compounds, furfural and HMF. These were present in larger amounts at 160 °C in the hydrochar, decreasing with T , and were washed out successfully (69–100%), while the phenolics in hydrochar increased with T , reaching high concentrations at 240 °C, and only 34% were removed through washing. This inverse relationship in the production and disappearance of the two aromatic groups was also confirmed by comparing the measured process water values to literature values and models from extensive kinetic studies by Reza et al. (2014) [30] and Berrero-López et al. (2018) [67]. The comparison highlighted that additional studies are required to develop practical reliable models for predicting trends in aromatic content in hydrochar from a wide range of feedstock. These results contribute to a better understanding of which aromatic compounds are easily removed by washing and how to combine this step with HTC operation. This leads to an interesting strategy to explore in future investigations for reducing the aromatic content of the hydrochar based on the combination of these experimental aromatic trends with the models to predict EY or HHV: (1) operate HTC at low process temperatures to reduce the production of hard-to-washout phenolic compounds and achieve high EY; (2) combine this with a minimal water washing step to remove the furanic compounds and undesired compounds in general; and (3) recycle the wash water back to the HTC system as make-up water for the next HTC run. This may be an economical way to maximize the EY and reduce unwanted substances in hydrochar and merits further investigation, especially in conjunction with a further post-processing step to improve the handling and transportation of hydrochar, such as agglomeration.

Agglomeration of hydrochars and potential applications for spherical pellets: The results of the initial testing showed that it is possible to use wet agglomeration techniques with additives and binder solution for producing spherical pellets from SCGs and their hydrochars with high mechanical stability. This is the first reported agglomeration experiment for SCG-hydrochars. The findings provide a fundamental basis for the agglomeration process with these hydrochars and requirements for hydrochar properties. Further investigation is required to match the selection of additives or binders to the hydrochar properties to achieve the desired physical properties of spherical pellets. The spherical pellets made from washed hydrochar (200 °C and 240 °C) with sizes between 2000–4000 μm are also interesting for soil amendments, since this is the size range for many fertilizer products and applicators. Future research with these pellets and their behavior in the soil can help determine the optimal size.

The outcomes of this study can be used as a basis for industries to develop a standard process to valorize spent coffee grounds, while scientists can use these results as a basis for future research on enhancing the physical and chemical properties of final hydrochar products, which can be applied either in soil or for energy purposes.

Supplementary Materials: The following supporting information can be downloaded at: <https://www.mdpi.com/article/10.3390/su16010338/s1>.

Author Contributions: Conceptualization, C.H.D., G.F. and J.A.L.; methodology, C.H.D., G.F., C.G. and J.A.L.; validation, C.H.D., G.F., C.G. and J.A.L.; formal analysis, C.H.D. and J.A.L.; investigation, C.H.D., G.F., C.G., M.G.F. and J.A.L.; resources, C.H.D., G.F. and J.A.L.; data curation, C.H.D., C.G.,

M.G.F. and J.A.L.; writing—original draft preparation, C.H.D., G.F., C.G. and J.A.L.; writing—review and editing, C.H.D., G.F., C.G. and J.A.L.; visualization, C.H.D. and J.A.L.; supervision, J.A.L.; project administration, J.A.L. All authors have read and agreed to the published version of the manuscript.

Funding: Financial support for C.H.D. came from the project CoffeeChar (FKZ 2819DOKA02), which is supported by funds of the Federal Ministry of Food and Agriculture (BMEL) based on a decision of the Parliament of the Federal Republic of Germany via the Federal Office for Agriculture and Food (BLE) under the innovation support program. Financial support for G.F. came from the National Recovery and Resilience Plan (NRRP), Mission 4 Component 2 Investment 1.5—Call for tender No.3277 published on 30 December 2021 by the Italian Ministry of University and Research (MUR) funded by the European Union—NextGenerationEU. Project Code ECS0000038—Project Title eINS Ecosystem of Innovation for Next Generation Sardinia—CUP F53C22000430001—Grant Assignment Decree No. 1056 adopted on 23 June 2022 by the Italian Ministry of Ministry of University and Research (MUR).

Institutional Review Board Statement: Not applicable.

Informed Consent Statement: Not applicable.

Data Availability Statement: The data presented in this study are available on request from the corresponding authors.

Acknowledgments: The authors gratefully acknowledge Christina Dornack (Institute of Waste Management and Circular Economy, Technische Universität Dresden) for her support in general, and specifically the handling, preparation, and storage of a large amount of wet SCGs in the laboratory. We would like to thank Giovanna Rehde and her team (Leibniz Institute of Agricultural Engineering and Bioeconomy, Potsdam) for their analytical support.

Conflicts of Interest: The authors declare no conflicts of interest.

References

1. ICO. Coffee Market Report July 2023. Available online: <https://icocoffee.org/> (accessed on 12 November 2022).
2. Kovalcik, A.; Obruca, S.; Marova, I. Valorization of spent coffee grounds: A review. *Food Bioprod. Process.* **2018**, *110*, 104–119. [CrossRef]
3. Bejenari, V.; Marcu, A.; Ipate, A.-M.; Rusu, D.; Tudorachi, N.; Anghel, I.; Şofran, I.-E.; Lisa, G. Physicochemical characterization and energy recovery of spent coffee grounds. *J. Mater. Res. Technol.* **2021**, *15*, 4437–4451. [CrossRef]
4. Fehse, F.; Kummich, J.; Schröder, H.-W. Influence of pre-treatment and variation of briquetting parameters on the mechanical refinement of spent coffee grounds. *Biomass Bioenergy* **2021**, *152*, 106201. [CrossRef]
5. De Freitas, C.P.M.; Marangon, B.B.; Pereira, E.G.; Renato, N.D.S. Exploring Spent Coffee Grounds Energy Potential In The Brazilian Scenario. *Eng. Agríc.* **2023**, *43*, e20220141. [CrossRef]
6. Santos, C.; Fonseca, J.; Aires, A.; Coutinho, J.; Trindade, H. Effect of different rates of spent coffee grounds (SCG) on composting process, gaseous emissions and quality of end-product. *Waste Manag.* **2017**, *59*, 37–47. [CrossRef] [PubMed]
7. de Bomfim, A.S.C.; de Oliveira, D.M.; Walling, E.; Babin, A.; Hersant, G.; Vaneckhaute, C.; Dumont, M.-J.; Rodrigue, D. Spent Coffee Grounds Characterization and Reuse in Composting and Soil Amendment. *Waste* **2022**, *1*, 2–20. [CrossRef]
8. Yang, J.; Zhao, Z.; Hu, Y.; Abbey, L.; Cesarino, I.; Goonetilleke, A.; He, Q. Exploring the Properties and Potential Uses of Biocarbon from Spent Coffee Grounds: A Comparative Look at Dry and Wet Processing Methods. *Processes* **2023**, *11*, 2099. [CrossRef]
9. Tun, M.M.; Raclavská, H.; Juchelková, D.; Růžičková, J.; Šafář, M.; Štrbová, K.; Gikas, P. Spent coffee ground as renewable energy source: Evaluation of the drying processes. *J. Environ. Manag.* **2020**, *275*, 111204. [CrossRef]
10. Susilayati, M.; Marwoto, P.; Priatmoko, S. Characterization of Spent Coffee Grounds in the Community as Supporting Materials for Renewable Energy. *J. Penelit. Pendidik. IPA* **2022**, *8*, 918–924. [CrossRef]
11. Turek, M.E.; Freitas, K.S.; Armindo, R.A. Spent coffee grounds as organic amendment modify hydraulic properties in a sandy loam Brazilian soil. *Agric. Water Manag.* **2019**, *222*, 313–321. [CrossRef]
12. Horgan, F.G.; Floyd, D.; Mundaca, E.A.; Crisol-Martínez, E. Spent Coffee Grounds Applied as a Top-Dressing or Incorporated into the Soil Can Improve Plant Growth While Reducing Slug Herbivory. *Agriculture* **2023**, *13*, 257. [CrossRef]
13. de Carvalho Ramos, N.; Campos, T.M.B.; de La Paz, I.S.; Machado, J.P.B.; Bottino, M.A.; Cesar, P.F.; De Melo, R.M. Microstructure characterization and SCG of newly engineered dental ceramics. *Dent. Mater.* **2016**, *32*, 870–878. [CrossRef] [PubMed]
14. Luna-Lama, F.; Rodríguez-Padrón, D.; Puente-Santiago, A.R.; Muñoz-Batista, M.J.; Caballero, A.; Balu, A.M.; Romero, A.A.; Luque, R. Non-porous carbonaceous materials derived from coffee waste grounds as highly sustainable anodes for lithium-ion batteries. *J. Clean. Prod.* **2019**, *207*, 411–417. [CrossRef]
15. Limousy, L.; Jeguirim, M.; Dutournié, P.; Kraiem, N.; Lajili, M.; Said, R. Gaseous products and particulate matter emissions of biomass residential boiler fired with spent coffee grounds pellets. *Fuel* **2013**, *107*, 323–329. [CrossRef]

16. Park, J.E.; Lee, G.B.; Jeong, C.J.; Kim, H.; Kim, C.G. Determination of Relationship between Higher Heating Value and Atomic Ratio of Hydrogen to Carbon in Spent Coffee Grounds by Hydrothermal Carbonization. *Energies* **2021**, *14*, 6551. [CrossRef]
17. Hu, Y.; Gallant, R.; Salaudeen, S.; Farooque, A.A.; He, S. Hydrothermal Carbonization of Spent Coffee Grounds for Producing Solid Fuel. *Sustainability* **2022**, *14*, 8818. [CrossRef]
18. Farru, G.; Dang, C.H.; Schultze, M.; Kern, J.; Cappai, G.; Libra, J.A. Benefits and Limitations of Using Hydrochars from Organic Residues as Replacement for Peat on Growing Media. *Horticulturae* **2022**, *8*, 325. [CrossRef]
19. Zhang, X.; Zhang, Y.; Ngo, H.H.; Guo, W.; Wen, H.; Zhang, D.; Li, C.; Qi, L. Characterization and sulfonamide antibiotics adsorption capacity of spent coffee grounds based biochar and hydrochar. *Sci. Total Environ.* **2020**, *716*, 137015. [CrossRef]
20. Santana, M.S.; Alves, R.P.; Santana, L.S.; Gonçalves, M.A.; Guerreiro, M.C. Structural, inorganic, and adsorptive properties of hydrochars obtained by hydrothermal carbonization of coffee waste. *J. Environ. Manag.* **2022**, *302*, 114021. [CrossRef]
21. Funke, A.; Ziegler, F. Hydrothermal carbonization of biomass: A summary and discussion of chemical mechanisms for process engineering. *Biofuels Bioprod. Biorefining* **2010**, *4*, 160–177. [CrossRef]
22. Libra, J.A.; Ro, K.S.; Kammann, C.; Funke, A.; Berge, N.D.; Neubauer, Y.; Titirici, M.-M.; Fühner, C.; Bens, O.; Kern, J.; et al. Hydrothermal carbonization of biomass residuals: A comparative review of the chemistry, processes and applications of wet and dry pyrolysis. *Biofuels* **2011**, *2*, 71–106. [CrossRef]
23. Ducey, T.F.; Collins, J.C.; Ro, K.S.; Woodbury, B.L.; Griffin, D.D. Hydrothermal carbonization of livestock mortality for the reduction of pathogens and microbially-derived DNA. *Front. Environ. Sci. Eng.* **2017**, *11*, 9. [CrossRef]
24. Román, S.; Nabais, J.M.V.; Laginhas, C.; Ledesma, B.; González, J.F. Hydrothermal carbonization as an effective way of densifying the energy content of biomass. *Fuel Process. Technol.* **2012**, *103*, 78–83. [CrossRef]
25. Kim, D.; Lee, K.; Bae, D.; Park, K.Y. Characterizations of biochar from hydrothermal carbonization of exhausted coffee residue. *J. Mater. Cycles Waste Manag.* **2017**, *19*, 1036–1043. [CrossRef]
26. Afolabi, O.O.D.; Sohail, M.; Cheng, Y.-L. Optimisation and characterisation of hydrochar production from spent coffee grounds by hydrothermal carbonisation. *Renew. Energy* **2020**, *147*, 1380–1391. [CrossRef]
27. Sermyagina, E.; Mendoza, C.; Deviatkin, I. Effect of hydrothermal carbonization and torrefaction on spent coffee grounds. *Agron. Res.* **2021**, *19*. [CrossRef]
28. Marzban, N.; Libra, J.A.; Hosseini, S.H.; Fischer, M.G.; Rotter, V.S. Experimental evaluation and application of genetic programming to develop predictive correlations for hydrochar higher heating value and yield to optimize the energy content. *J. Environ. Chem. Eng.* **2022**, *10*, 108880. [CrossRef]
29. Moloeznik Paniagua, D.; Libra, J.A.; Rotter, V.S.; Ro, K.S.; Fischer, M.; Linden, J. Enhancing Fuel Properties of Napier Grass via Carbonization: A Comparison of Vapothermal and Hydrothermal Carbonization Treatments. *Agronomy* **2023**, *13*, 2881. [CrossRef]
30. Reza, M.T.; Wirth, B.; Lüder, U.; Werner, M. Behavior of selected hydrolyzed and dehydrated products during hydrothermal carbonization of biomass. *Bioresour. Technol.* **2014**, *169*, 352–361. [CrossRef]
31. Borrero-López, A.M.; Masson, E.; Celzard, A.; Fierro, V. Modelling the production of solid and liquid products from the hydrothermal carbonisation of two biomasses. *Ind. Crops Prod.* **2020**, *151*, 112452. [CrossRef]
32. Erdogan, E.; Atila, B.; Mumme, J.; Reza, M.T.; Toptas, A.; Elibol, M.; Yanik, J. Characterization of products from hydrothermal carbonization of orange pomace including anaerobic digestibility of process liquor. *Bioresour. Technol.* **2015**, *196*, 35–42. [CrossRef]
33. Ipiates, R.P.; de la Rubia, M.A.; Diaz, E.; Mohedano, A.F.; Rodriguez, J.J. Integration of Hydrothermal Carbonization and Anaerobic Digestion for Energy Recovery of Biomass Waste: An Overview. *Energy Fuels* **2021**, *35*, 17032–17050. [CrossRef]
34. EPA. Integrated Risk Information System: Phenol. Available online: <https://www.epa.gov/iris> (accessed on 11 December 2023).
35. Downs, J.; Wills, B. Phenol Toxicity. Phenol Toxicity. [Updated 13 March 2023]. In *StatPearls*; StatPearls Publishing: Treasure Island, FL, USA, 2023. Available online: <https://www.ncbi.nlm.nih.gov/books/NBK542311/> (accessed on 13 October 2023).
36. Bargmann, I.; Rillig, M.C.; Buss, W.; Kruse, A.; Kuecke, M. Hydrochar and Biochar Effects on Germination of Spring Barley. *J. Agron. Crop Sci.* **2013**, *199*, 360–373. [CrossRef]
37. Karatas, O.; Khataee, A.; Kalderis, D. Recent progress on the phytotoxic effects of hydrochars and toxicity reduction approaches. *Chemosphere* **2022**, *298*, 134357. [CrossRef] [PubMed]
38. Chakrabarti, S.; Dicke, C.; Kalderis, D.; Kern, J. Rice husks and their hydrochars cause unexpected stress response in the nematode *Caenorhabditis elegans*: Reduced transcription of stress-related genes. *Environ. Sci. Pollut. Res.* **2015**, *22*, 12092–12103. [CrossRef] [PubMed]
39. Fan, G.; Tong, F.; Zhang, W.; Shi, G.; Chen, W.; Liu, L.; Li, J.; Zhang, Z.; Gao, Y. The effect of organic solvent washing on the structure of hydrochar-based dissolved organic matters and its potential environmental toxicity. *Environ. Sci. Pollut. Res.* **2021**, *28*, 26584–26594. [CrossRef] [PubMed]
40. Cervera-Mata, A.; Lara, L.; Fernández-Arteaga, A.; Ángel Rufián-Henares, J.; Delgado, G. Washed hydrochar from spent coffee grounds: A second generation of coffee residues. Evaluation as organic amendment. *Waste Manag.* **2021**, *120*, 322–329. [CrossRef]
41. Hoekman, S.K.; Broch, A.; Felix, L.; Farthing, W. Hydrothermal carbonization (HTC) of loblolly pine using a continuous, reactive twin-screw extruder. *Energy Convers. Manag.* **2017**, *134*, 247–259. [CrossRef]
42. Mohammadi, A. Overview of the Benefits and Challenges Associated with Pelletizing Biochar. *Processes* **2021**, *9*, 1591. [CrossRef]
43. Colantoni, A.; Paris, E.; Bianchini, L.; Ferri, S.; Marcantonio, V.; Carnevale, M.; Palma, A.; Civitaresse, V.; Gallucci, F. Spent coffee ground characterization, pelletization test and emissions assessment in the combustion process. *Sci. Rep.* **2021**, *11*, 5119. [CrossRef]

44. Woo, D.-G.; Kim, S.H.; Kim, T.H. Solid Fuel Characteristics of Pellets Comprising Spent Coffee Grounds and Wood Powder. *Energies* **2021**, *14*, 371. [CrossRef]
45. Mort, P.R. Scale-up of binder agglomeration processes. *Powder Technol.* **2005**, *150*, 86–103. [CrossRef]
46. Briens, L.; Bowden-Green, B. A comparison of drum granulation of biochars. *Powder Technol.* **2019**, *343*, 723–732. [CrossRef]
47. Jones, B.; Nachtshiem, C.J. A Class of Three-Level Designs for Definitive Screening in the Presence of Second-Order Effects. *J. Qual. Technol.* **2011**, *43*, 1–15. [CrossRef]
48. Montgomery, D.C. *Design and Analysis of Experiments*, 8th ed.; Wiley: Hoboken, NJ, USA, 2012; ISBN 978-1-118-14692-7.
49. Heidari, M.; Norouzi, O.; Salaudeen, S.; Acharya, B.; Dutta, A. Prediction of Hydrothermal Carbonization with Respect to the Biomass Components and Severity Factor. *Energy Fuels* **2019**, *33*, 9916–9924. [CrossRef]
50. Ruiz, H.A.; Galbe, M.; Garrote, G.; Ramirez-Gutierrez, D.M.; Ximenes, E.; Sun, S.-N.; Lachos-Perez, D.; Rodríguez-Jasso, R.M.; Sun, R.-C.; Yang, B.; et al. Severity factor kinetic model as a strategic parameter of hydrothermal processing (steam explosion and liquid hot water) for biomass fractionation under biorefinery concept. *Bioresour. Technol.* **2021**, *342*, 125961. [CrossRef]
51. ISO 17225-8:2023; Solid Biofuels. International Organization for Standardization: Geneva, Switzerland, 2023.
52. Özer, M.; Basha, O.M.; Morsi, B. Coal-Agglomeration Processes: A Review. *Int. J. Coal Prep. Util.* **2017**, *37*, 131–167. [CrossRef]
53. Lu, X.; Pellechia, P.J.; Flora, J.R.V.; Berge, N.D. Influence of reaction time and temperature on product formation and characteristics associated with the hydrothermal carbonization of cellulose. *Bioresour. Technol.* **2013**, *138*, 180–190. [CrossRef]
54. Nizamuddin, S.; Baloch, H.A.; Griffin, G.J.; Mubarak, N.M.; Bhutto, A.W.; Abro, R.; Mazari, S.A.; Ali, B.S. An overview of effect of process parameters on hydrothermal carbonization of biomass. *Renew. Sustain. Energy Rev.* **2017**, *73*, 1289–1299. [CrossRef]
55. Ro, K.S.; Flora, J.R.V.; Bae, S.; Libra, J.A.; Berge, N.D.; Álvarez-Murillo, A.; Li, L. Properties of Animal-Manure-Based Hydrochars and Predictions Using Published Models. *ACS Sustain. Chem. Eng.* **2017**, *5*, 7317–7324. [CrossRef]
56. Wüst, D.; Correa, C.R.; Jung, D.; Zimmermann, M.; Kruse, A.; Fiori, L. Understanding the influence of biomass particle size and reaction medium on the formation pathways of hydrochar. *Biomass Convers. Biorefin.* **2020**, *10*, 1357–1380. [CrossRef]
57. Arauzo, P.J.; Lucian, M.; Du, L.; Olszewski, M.P.; Fiori, L.; Kruse, A. Improving the recovery of phenolic compounds from spent coffee grounds by using hydrothermal delignification coupled with ultrasound assisted extraction. *Biomass Bioenergy* **2020**, *139*, 105616. [CrossRef]
58. Shen, H.; Luo, Z.; Xiong, R.; Liu, X.; Zhang, L.; Li, Y.; Du, W.; Chen, Y.; Cheng, H.; Shen, G.; et al. A critical review of pollutant emission factors from fuel combustion in home stoves. *Environ. Int.* **2021**, *157*, 106841. [CrossRef] [PubMed]
59. Pereira, A.P.; Woodman, T.J.; Chuck, C.J. An integrated biorefinery to produce 5-(hydroxymethyl)furfural and alternative fuel precursors from macroalgae and spent coffee grounds. *Sustain. Energy Fuels* **2021**, *5*, 6189–6196. [CrossRef]
60. Kruse, A.; Funke, A.; Titirici, M.-M. Hydrothermal conversion of biomass to fuels and energetic materials. *Curr. Opin. Chem. Biol.* **2013**, *17*, 515–521. [CrossRef]
61. Park, J.; Nkurunziza, D.; Roy, V.C.; Ho, T.C.; Kim, S.; Lee, S.; Chun, B. Pretreatment processes assisted subcritical water hydrolysis for valorisation of spent coffee grounds. *Int. J. Food Sci. Technol.* **2022**, *57*, 5090–5101. [CrossRef]
62. Upadhyay, R.; Mohan Rao, L.J. An Outlook on Chlorogenic Acids—Occurrence, Chemistry, Technology, and Biological Activities. *Crit. Rev. Food Sci. Nutr.* **2013**, *53*, 968–984. [CrossRef]
63. Clifford, M.N. Miscellaneous phenols in foods and beverages—nature, occurrence and dietary burden. *J. Sci. Food Agric.* **2000**, *80*, 1126–1137. [CrossRef]
64. Murkovic, M.; Bornik, M.-A. Formation of 5-hydroxymethyl-2-furfural (HMF) and 5-hydroxymethyl-2-furoic acid during roasting of coffee. *Mol. Nutr. Food Res.* **2007**, *51*, 390–394. [CrossRef]
65. Liu, Q.; Zhou, P.; Luo, P.; Wu, P. Occurrence of Furfural and Its Derivatives in Coffee Products in China and Estimation of Dietary Intake. *Foods* **2023**, *12*, 200. [CrossRef]
66. Panigrahy, N.; Priyadarshini, A.; Sahoo, M.M.; Verma, A.K.; Daverey, A.; Sahoo, N.K. A comprehensive review on eco-toxicity and biodegradation of phenolics: Recent progress and future outlook. *Environ. Technol. Innov.* **2022**, *27*, 102423. [CrossRef]
67. Borrero-López, A.M.; Masson, E.; Celzard, A.; Fierro, V. Modelling the reactions of cellulose, hemicellulose and lignin submitted to hydrothermal treatment. *Ind. Crops Prod.* **2018**, *124*, 919–930. [CrossRef]
68. Al-Wabel, M.I.; Rafique, M.I.; Ahmad, M.; Ahmad, M.; Hussain, A.; Usman, A.R.A. Pyrolytic and hydrothermal carbonization of date palm leaflets: Characteristics and ecotoxicological effects on seed germination of lettuce. *Saudi J. Biol. Sci.* **2019**, *26*, 665–672. [CrossRef] [PubMed]
69. Johansen, A.; Schæfer, T. Effects of interactions between powder particle size and binder viscosity on agglomerate growth mechanisms in a high shear mixer. *Eur. J. Pharm. Sci.* **2001**, *12*, 297–309. [CrossRef]
70. Incitec Pivot. Density and Sizing Report 2019. Available online: <https://www.incitecpivotfertilisers.com.au/> (accessed on 13 November 2023).

Disclaimer/Publisher’s Note: The statements, opinions and data contained in all publications are solely those of the individual author(s) and contributor(s) and not of MDPI and/or the editor(s). MDPI and/or the editor(s) disclaim responsibility for any injury to people or property resulting from any ideas, methods, instructions or products referred to in the content.